



AEROSOL LOADING OVER THE SOUTH AFRICAN HIGHVELD

Thomas Aquinas Bigala

A dissertation submitted to the Faculty of Science, University of the Witwatersrand, in fulfilment of the requirements for the degree of Master of Science in Environmental Sciences

October, 2008

ABSTRACT

The Highveld region of South Africa contributes substantially to the aerosol loading over southern Africa because of its importance as an industrial, mining and farming base. Aerosols affect climate by absorbing or reflecting incoming solar radiation, and by affecting cloud microphysics, cloud albedo and precipitation. The physical and optical properties of industrial/urban aerosols over the Highveld region of South Africa were analysed during a 32-day winter sampling period (21 May to 21 June) in 2002; a 32-day summer sampling period (21 October to 21 November) in 2002, and a second 32-day winter sampling period (19 May to 19 June) in 2003. Synoptic circulation systems were examined in as far as they affect the horizontal transport of aerosols over the Highveld region. Measurements of aerosol optical thickness (AOT) from the ground to the top of the atmosphere and aerosol size distribution characteristics over the Highveld region were taken using hand-held hazemeters and a CIMEL sun photometer. The AOT observed over the region during the winter 2002 and 2003 sampling periods and during the summer 2002 sampling period indicated high turbidity. In the 2002 winter sampling period, the AOT_{530nm} ranged between 0.05 to 0.7 with an average of 0.14. In the 2002 summer sampling period, the AOT_{530nm} ranged between 0.05 to 0.6, with an average of 0.24. In the 2003 winter sampling period, the AOT_{500nm} ranged between 0.06 to 0.6, with an average of 0.21. The Ångström exponent value had a wide range, 0.8 to 2.4 in the 2002 winter and summer sampling periods and also in the 2003 winter sampling period, indicating that a range of particle sizes was present over the Highveld region. The Ångström exponent values obtained were derived from the influences of Aeolian dust, coarse-mode industrial particles and, to a small extent, fine-mode biomass-burning aerosols. Case studies, based on trajectory analysis and meteorology of the sampling area, were made of the aerosols emanating from the township sites during each of the three sampling periods to observe the build-up and dispersion of aerosols at that time.

KEY WORDS:

Aerosol loading, hand-held hazemeter, CIMEL sun photometer, Ångström exponent values, aerosol optical thickness values.

DECLARATION

I declare that this dissertation is my own, unaided work except where acknowledged. It is being submitted for the Degree of Master of Science in the University of the Witwatersrand, Johannesburg. It has not been submitted before for any degree or examination in any other University.

Thomas Aquinas Bigala

October 2008

To my God in Heaven for who He is and what He is doing in my life.

Blessed is the man who dwells not in the counsel of the ungodly, nor stands in the way of sinners, nor sits in the seat of the scornful. But his delight is in the Word of the Lord, and in the Word does he meditate day and night. For he is like a tree planted by the rivers of water, and he shall bring forth his seed in his season.

(The book of Psalms 1:1-3)

To my parents, who made enormous sacrifices to bring me up
to be the person I am today.

PREFACE

Tropospheric aerosols are highly efficient in interacting with solar radiation in the visible and near infrared spectrum. They directly perturb the spatial distribution of solar energy by light absorption and by back-scattering radiation to space. Aerosols may reduce the degree of global warming resulting from the increase of greenhouse gases in the atmosphere. They directly impact the radiative balance of Earth through a net increase of its albedo, particularly over the oceans. Aerosols can also act as cloud condensation nuclei, increasing the number of droplets in clouds, which tends to decrease the mean droplet size and may increase the cloud albedo, depending on the aerosol absorption and cloud optical thickness. The variety of aerosol sources, both natural and anthropogenic, and the short lifetime of aerosols (5 to 10 days) result in a spatially heterogeneous aerosol field. The estimates of magnitude of these effects, however, are poorly constrained because there is a limited knowledge of the processes that control the distributions as well as the physical, chemical and optical properties of aerosols.

Interest in regional aerosol monitoring over southern Africa has increased following the recognition of the consequences of the layering of the atmosphere on the accumulation of biogenic and anthropogenic products throughout the troposphere. Whereas both surface and elevated absolutely stable layers may lead to locally high concentrations of air pollution in the troposphere, it is the elevated layers which play an important role in controlling medium- to long-range transport and re-circulation of aerosols and trace gases.

It may be hypothesised that there is substantial atmospheric aerosol loading over the Highveld region of South Africa. The Highveld region of Mpumalanga and Gauteng

is the major industrial area in South Africa and is the source region for emissions to the atmosphere of sulphur, carbon, nitrogen and their associated oxides. Coupled with these emissions is the high incidence of biomass burning from farms and human settlements. Biomass burning during the late dry season is due to the seasonal oscillation between a wet season of biomass production and a dry season. The persistent formation of elevated absolutely stable layers in the atmosphere over the Highveld region contributes to the pollution problem by preventing the rapid dispersal of aerosols. Existing literature has paid much attention to how aerosols are transported from the Highveld towards the Lowveld regions of South Africa.

The spatial distribution of aerosol loading, as well as the seasonal variation and magnitude of the aerosol load over the Highveld, is discussed in this dissertation. Backward trajectory analysis was carried out to ascertain the origin of the aerosols. Data collection took place over three 32-day periods in 2002 and 2003: May and June (winter) in 2002 and 2003 and October and November (summer) 2002.

Aim and objective of the research

The aim of this study was to measure the spatial and temporal variation of aerosols and relate them to air pollution source emissions over the Highveld region of South Africa.

Structure of the dissertation

This dissertation is divided into five chapters. **Chapter 1** provides background information relating to aerosol optical characteristics, specifically looking at aerosol optical properties and sun-photometry, and states the hypothesis to be tested. **Chapter 2** presents data collection and analytical methodologies. **Chapter 3** contains a discussion of aerosol optical thickness and its characteristics over the Highveld region, and the associated relationships between the sites. This chapter also presents a comparison between the Ångström parameter and water vapour content.

Chapter 4 presents a synoptic interpretation of the data and discussion of atmospheric transport and backward trajectory analyses to examine aerosol transport to the sampling sites. This chapter also contains case studies taken from the sampling periods, based on trajectory analysis and meteorology of the sampling area, that was made of the aerosols emanating from the township sites during each of the three sampling periods to observe the build-up and dispersion of the aerosols during each sampling period. Township sites were chosen because of their unique characteristic of being densely populated, under-resourced residential areas. **Chapter 5** presents the summary and conclusions of the study.

Parts of this research have been presented at the South African Society for Atmospheric Scientists and at the National Association for Clean Air Conferences for the years 2002 to 2006.

ACKNOWLEDGEMENTS

- I would like to thank Dr S Piketh, for his untiring guidance and valuable assistance.
- Dr Tal Freiman for her willing inputs.
- My prayer partner, Ignatius - thank you so much.
- Ms L Frewin and Ms S Bhailall for their, diligence and encouragement.
- Mss L Raymond for her support, warmth and love.
- The entire Climatology Research Group for their encouragement, especially during trying times.
- Funding for this project was provided by the Climatology Research Group and Eskom TSI.
- Jeannette Menasce is acknowledged for her assistance in proof-reading and correcting this dissertation.

CONTENTS

ABSTRACT	i
KEY WORDS:	ii
DECLARATION	iii
PREFACE	v
Aim and objective of the research	vi
Structure of the dissertation	vi
ACKNOWLEDGEMENTS	viii
CONTENTS	ix
LIST OF FIGURES	xii
LIST OF TABLES	xvi
ABBREVIATIONS, ACRONYMS AND GLOSSARY	xvii
CHAPTER 1: INTRODUCTION AND LITERATURE REVIEW	1
Aerosol optical properties	3
• <i>Extinction or attenuation</i>	<i>3</i>
• <i>Aerosol size</i>	<i>3</i>
• <i>Ångström exponent formula for aerosols</i>	<i>4</i>
Aerosols and their source regions within southern Africa	4
• <i>The Highveld</i>	<i>5</i>
Literature review	6
• <i>Aerosols</i>	<i>6</i>
• <i>Effects of anthropogenic aerosols</i>	<i>11</i>

•	<i>South African atmospheric conditions</i>	12
CHAPTER 2: DATA AND METHODOLOGY		16
Highveld site description		16
Data collection		20
•	<i>CIMEL sun photometer</i>	21
•	<i>The hazemeter</i>	22
Trajectory analysis		26
Statistical analysis		28
Data recovery		28
Surface synoptic charts		31
 CHAPTER 3: DISTRIBUTION OF AEROSOLS OVER THE HIGHVELD		 32
Seasonal variation of AOT over the Highveld		32
•	<i>Variation between township, industrial/urban, and agricultural sites</i>	34
•	<i>Township sites</i>	34
•	<i>Industrial/urban sites</i>	36
•	<i>Agricultural sites</i>	37
•	<i>Wind speed and wind direction during the 2002 sampling periods</i>	39
Spatial variation in AOT_{530nm} across the Highveld		41
Correlation of aerosol optical thickness between sites		43
•	<i>Township sites</i>	43
•	<i>Industrial/urban sites</i>	45
•	<i>Agricultural sites</i>	47
Seasonal variation in aerosol size across the Highveld		49

Comparison of Ångström exponent in winter and summer between township, industrial/urban and agricultural sites	50
• <i>Township sites</i>	<i>50</i>
• <i>Industrial/urban sites</i>	<i>52</i>
• <i>Agricultural sites</i>	<i>53</i>
• <i>Ångström exponent and precipitable water vapour content in winter and summer</i>	<i>55</i>
CHAPTER 4: SYNOPTIC CIRCULATION AND ATMOSPHERIC TRANSPORT	58
Frequency of occurrence of atmospheric transport systems during the Highveld Haze Project (2002 to 2003).....	58
Atmospheric transport over the Highveld during the winter and summer 2002 sampling periods selected using case studies from the township sites	60
• <i>The selected case studies have been used to show how the combination of cold fronts versus anti-cyclonic weather phenomena brought about low and high AOT loading over the township sites throughout the sampling periods.</i>	<i>60</i>
• <i>Winter 2002.....</i>	<i>60</i>
• <i>Summer 2002.....</i>	<i>68</i>
CHAPTER 5: SUMMARY AND CONCLUSION	74
REFERENCES	77

LIST OF FIGURES

Figure 1.1:	The main transport pathways associated with different circulation types over southern Africa	14
Figure 2.1:	Location of hazemeters over the Highveld region during 2002 and 2003	17
Figure 2.2:	Grade 10 and 11 learners using a hazemeter during the launch of the Highveld haze project.....	19
Figure 2.3:	Schematic diagram of an extinction measuring apparatus	20
Figure 2.4:	The CIMEL sun photometer situated at the University of the Witwatersrand.....	22
Figure 2.5:	A hazemeter used in the research	24
Figure 2.6:	Three-day transport of atmospheric particulates with different circulation systems over South Africa.....	27
Figure 2.7:	Data collected as a percentage during a) winter 2002, b) winter 2003 and c) summer 2002	30
Figure 3.1:	Frequency of occurrence of daily aerosol optical thickness during summer 2002 (AOT_{530nm}), winter 2002 (AOT_{530nm}) and winter 2003 (AOT_{500nm}) for all sites over the Highveld region.....	33
Figure 3.2:	Frequency of occurrence of daily average $AOT_{530 nm}$ for township sites during the winter 2002 sampling period.....	35
Figure 3.3:	Frequency of occurrence of daily average $AOT_{530 nm}$ for township sites during the summer 2002 sampling period	35
Figure 3.4:	Frequency of occurrence of daily AOT_{530nm} for industrial/urban sites during the winter 2002 sampling period.....	36
Figure 3.5:	Frequency of occurrence of daily AOT_{530nm} for industrial/urban sites during the summer 2002 sampling period.....	36

Figure 3.6:	Frequency of occurrence of daily AOT _{530nm} for agricultural sites in the winter 2002 sampling period.....	37
Figure 3.7a:	Frequency of occurrence of daily AOT _{530nm} for agricultural sites during the summer 2002 sampling period.....	38
Figure 3.7b:	Daily AOT _{530nm} for Bela Bela during the summer 2002 sampling period.....	38
Figure 3.8:	Hourly average wind roses depicting the prevailing winds in winter 2002 calculated at the OR Tambo International Airport.....	39
Figure 3.9:	Hourly average wind roses depicting the prevailing winds in summer 2002 calculated at the OR Tambo International Airport.....	40
Figure 3.10:	Spatial variation of AOT _{530nm} over the Highveld region in winter 2002.....	42
Figure 3.11:	Spatial variation of AOT _{530nm} over the Highveld region in summer 2002.....	43
Figure 3.12:	Map of the township sites showing their positions relative to each other.....	44
Figure 3.13:	Map of the industrial/urban sites showing their positions relative to each other.....	46
Figure 3.14:	Map of the agricultural sites showing their positions relative to each other.....	48
Figure 3.15:	Frequency of occurrence of Ångström exponent in winter and summer 2002 and winter 2003.....	50
Figure 3.16:	Frequency of occurrence of Ångström exponent in winter 2002 for township sites.....	51
Figure 3.17:	Frequency of occurrence of Ångström exponent in summer 2002 for township sites.....	51
Figure 3.18:	Frequency of occurrence histograms of Ångström exponent in winter 2002 for industrial/urban sites.....	52
Figure 3.19:	Frequency of occurrence histograms of Ångström exponent in summer 2002 for industrial/urban sites.....	53
Figure 3.20:	Frequency of occurrence histograms of Ångström exponent in winter 2002 for agricultural sites.....	54

Figure 3.21:	Frequency of occurrence histograms of Ångström exponent in summer 2002 at agricultural sites.....	54
Figure 3.22:	Ångström exponent versus water vapour variability in a) winter 2002 and b) summer 2002	56
Figure 4.1:	Synoptic surface frequency of occurrence over the Highveld region in winter 2002, winter 2003 and summer 2002.....	59
Figure 4.2:	Surface weather charts on a) 10 June, b) 17 June and c) 21 June 2002 showing conditions conducive for AOT build-up over township sites	61
Figure 4.3:	Surface weather charts on a) 12 June and b) 14 June 2002 showing cold front conditions over township sites	62
Figure 4.4:	Aerosol optical thickness measurements for winter 2002 sampling period over township sites	62
Figure 4.5:	Four-day backward trajectory in winter 2002 showing transport into the Highveld on a) 10 June, b) 17 June and c) 21 June at 800, 700 and 500 hPa under conditions favourable for AOT build-up.....	64
Figure 4.6:	Aerosol optical thickness measurements for winter 2003 over township sites	65
Figure 4.7:	Surface weather charts on a) 2 June, b) 5 June, c) 7 June and d) 9 June 2003 showing a cold front over the Highveld region	66
Figure 4.8:	Four-day backward trajectory in winter 2003 showing transport into township sites for the period 2 to 9 June at 800, 700 and 500 hPa under low AOT conditions	67
Figure 4.9:	Aerosol optical thickness measurements for the summer 2002 sampling period	68
Figure 4.10:	Surface weather charts on 28 October 2002 showing a shallow low pressure system over the Highveld region.....	69
Figure 4.11:	Four-day backward trajectory in summer 2002 showing transport into the Highveld for the period 27 to 30 October at 800, 700 and 500 hPa	70

Figure 4.12: Surface weather charts on a) 11 November, b) 13 November, 2002 showing a shallow low pressure system over the Highveld region..... 71

Figure 4.13: Four-day backward trajectory in summer 2002 showing transport into the Highveld for the period 11 to 13 November at 800, 700 and 500 hPa under low AOT conditions 72

LIST OF TABLES

Table 1.1:	Energy sector carbon emission intensity and carbon emission per caput for 1995.....	5
Table 2.1:	Location and classification of hazemeter sites over the Highveld region.....	18
Table 2.2:	Spectral bands used to measure aerosol optical thickness over land	25
Table 2.3:	Typical ranges for aerosol optical thickness	25
Table 3.1:	Correlation matrices at AOT _{530nm} measured at township sites in winter and summer 2002	45
Table 3.2:	Correlation matrices at AOT _{530nm} measured at industrial/urban sites in winter and summer 2002	47
Table 3.3:	Correlation matrices at AOT _{530nm} measured at agricultural sites in winter and summer 2002	48

ABBREVIATIONS, ACRONYMS AND GLOSSARY

AERONET	Aerosol Robotic Network
Agricultural sites	Aerosol monitoring sites situated in Bela-Bela [formerly Warmbaths], Elias Motsaledi [formerly Groblersdal] and Marble Hall
AOT	Aerosol optical thickness (also referred to as aerosol optical depth in some literature)
ASL	Above sea level
HYSPLIT_4	Hybrid Single-Particle Lagrangian Integrated Trajectory
Industrial/urban sites	Aerosol monitoring sites situated in Johannesburg, Middelburg, Pretoria, Rustenburg, Secunda, Springs, Vereeniging and Witbank
NASA	National Aeronautical Space Administration
nm	nanometer (10^{-9} m)
NOAA	National Oceanic and Atmospheric Administration (Air Resources Laboratory)
OECD	Organisation of Economic Co-operation and Development (countries)
SAFARI 2000	South African Regional Science Initiative 2000
SO ₂	Sulphur dioxide
Township sites	Aerosol monitoring sites situated at schools in Bethal, Ermelo, Kinross, Mashishing [formerly Lydenburg], Sebokeng, Soweto and Standerton
á	Ångström exponent
µm	micrometer (10^{-6} m)

CHAPTER 1:

INTRODUCTION AND LITERATURE REVIEW

A discussion of the factors governing aerosol optical thickness will be given in this chapter. The major findings of research around the world in general, and specifically in South Africa, pertaining to aerosol loadings will be considered.

Humans have always influenced their environment. However, since the beginning of the Industrial Revolution, from the mid-18th Century, the impact of human activities has begun to extend on continental and global scales. In particular, those human activities involving the combustion of fossil fuels (for industrial or domestic usage and biomass burning), produce greenhouse gases and aerosols. Aerosols are tiny liquid and solid particles suspended in air. Most aerosols occur naturally, originating from volcanoes, dust storms, forest- and grassland fires, vegetation and sea spray. These affect the composition of the atmosphere (IPCC, 2001). The anthropogenic contribution to the atmospheric aerosol loading is not known, neither is the level of the total aerosol loading currently defined (Andreae, 1996). Aerosols made by human activities – when averaged across the globe – presently account for approximately 10 % of the aerosol mass in the atmosphere (NASA, 2002). A higher proportion of the anthropogenic percentage is concentrated in the northern hemisphere, especially downwind of industrial sites, slash-and-burn agricultural regions, and overgrazed grasslands.

Regional interest in aerosol monitoring over the southern Africa continent has increased following the recent recognition of large-scale recirculation patterns over the sub-continent and the existence of absolutely stable layers that allow for the

accumulation of a substantial quantity of aerosol loading over the sub-continent. The consequences of this stable layering of the atmosphere – causing the accumulation of anthropogenic and biogenic products throughout the troposphere – are considerable (Freiman and Tyson, 2000). Both surface and elevated absolutely stable layers may lead to local high concentrations of air pollution in the troposphere. It is these elevated layers that play an important role in controlling medium- to long-range transport and recirculation of aerosols and trace gases (Tyson and Preston-Whyte, 2000; Garstang *et al.*, 1996).

Aerosol generation processes in southern Africa are associated with wind-blown dust, industrial emissions (sulphate, nitrate and organic particle production), biomass burning (savannah fires, agricultural waste combustion and domestic biofuel combustion), and sea salt spray (Piketh *et al.*, 1999). The South African Highveld is a major source of primary pollutants. The high-stack policy used by both Eskom (electricity generation) and Sasol (fuel from coal processing) appears to have succeeded in controlling ground-level concentrations of both primary and secondary pollutants. However, this high-stack policy, together with the meteorological conditions, has resulted in the development of elevated layers with high concentrations of secondary pollutants (Piketh *et al.*, 1999). Downwind transport of these aerosols occurs over long distances, with multi-scale recirculation of material frequently occurring before its subsequent transport offshore towards the Indian Ocean (Piketh *et al.*, 1999; Garstang *et al.*, 1996; Tyson, 1999). The combination of emission sources over the South African Highveld concentrates both gaseous and aerosol pollutants throughout the year (Held *et al.*, 1996).

Aerosol optical properties

Extinction or attenuation

In optics, the Beer-Lambert law, also known as Beer's law, is an empirical relationship that relates the absorption of light, I , to the properties of the material through which the light is travelling. In terms of this law,

$$I = I_0 \exp(-\tau m) \quad [1.1]$$

where I_0 is the intensity of the same light source seen through the same volume without scattering particles and τ (nm) is the total atmospheric optical thickness (sum of the optical thickness of molecules, gases and aerosols). The optical air mass, m (cm^{-3}), is a measure of the slant path traversed by the direct solar beam reaching the ground, and is roughly proportional to the inverse of the cosine of the solar zenith angle. The extinction of light by aerosol particles and gases is due to two processes: firstly, by elastic scattering (in which part of the light from a beam is deflected towards other directions) where the light energy is conserved; and secondly, by absorption, where the photons transfer their energy to the particle (increasing the internal energy of the particle and eventually the energy of the surrounding medium) (Iqbal, 1983).

Aerosol size

Aerosols larger than $\sim 1 \mu\text{m}$ in diameter (coarse particles) are derived from soil dust and sea salt (Raes *et al.*, 1995). Aerosols with diameters $< 1 \mu\text{m}$ (fine particles) are formed mainly by combustion or the chemical conversion of gaseous precursors into liquid or solid products (gas-to-particle conversion). Aerosol size is the most important parameter used in characterising the physical properties of aerosols (Hinds, 1982). The fine fraction aerosols are primary influences in terms of radiative forcing, having low impaction efficiencies and sedimentation velocities, and a high scattering

efficiency. The fine fraction aerosols can travel long distances and be taken up to higher altitudes where they are able to interact with clouds (Raes *et al.*, 1995).

Ångström exponent formula for aerosols

The spectral relationship between the logarithm of aerosol optical thickness (AOT) and the logarithm of wavelength is approximately linear (Ångström, 1961). The slope of this relationship across the visible spectral region has become an important parameter, demonstrating average aerosol dimensions in the sub-micrometer to the super-micrometer particle size range (O'Neill *et al.*, 2001). Studies on AOT and its spectral dependence rely on the Ångström wavelength exponent, which can be derived from the formula:

$$\tau_a = \beta \lambda^{-\alpha} \quad [1.2]$$

Where β is the Ångström turbidity coefficient and λ (μm) is the wavelength in microns of the corresponding AOT τ_a values. The above equation is ratioed at two different wavelengths and the logarithm is taken of the typical values of the Ångström wavelength exponent. The Ångström wavelength exponent ranges from >2.0 for fresh smoke particles, which are dominated by accumulation-mode aerosols, to nearly zero for high optical thickness desert dust dominated by coarse-mode aerosols (Holben *et al.*, 1998). Although the Ångström exponent gives average integrated aerosol size, it should be noted that the atmosphere is made up of varying sizes of aerosols in different concentrations and the amount of solar radiation attenuated by aerosols is strongly dependent on the aerosol size distribution.

Aerosols and their source regions within southern Africa

Southern Africa is a largely underdeveloped region, with concentrations of intensive industrial activity, particularly in South Africa, occurring locally. Previous source region studies have identified four major contributing source types of regional aerosols: mineral soil dust, marine aerosols, aerosols from industrial emissions and

biomass burning particles (mainly north of 20° S) (Annegarn *et al.*, 1992; Piketh, 1995; Piketh *et al.*, 1996; Salma *et al.*, 1992; Maenhaut *et al.*, 1996). Biomass burning and industrial emissions have been shown to have the greatest potential for inducing environmental and climatic change (Charlson *et al.*, 1990; Andreae, 1996).

The Highveld

South Africa is one of the most carbon emission-intensive countries in the world, due to an energy-intensive economy and a high dependency on coal as a source of energy. South African per caput carbon emissions are higher than those of many European countries and near the levels of the Organisation of Economic Cooperation and Development (OECD) countries (Table 1.1).

Table 1.1: Energy sector carbon emission intensity and carbon emission per caput for 1995

Country / Region	CO₂ tonnes/caput	CO₂ / GDP* kg	CO₂ GDP PPP** kg / 1995 PPP US\$
South Africa	8.23	2.11	0.96
Africa	0.09	1.28	0.49
Non-OECD	2.24	1.79	0.66
OECD	10.96	0.46	0.52
World	3.88	0.71	0.58
*GDP = Gross Domestic Product **PPP = Purchasing Power Parity			
Source: OECD, 1999:8.			

This high carbon emission level is partly a result of energy intensive sectors (such as mining and iron, steel, aluminium and ferrochrome processing and manufacturing) that are not only important to the local economy, but also make up a large proportion

of South African exports (Visser *et al.*, 1999; Spalding-Fecher *et al.*, 2000). The same authors note that plentiful supplies of inexpensive coal have supported the development of large-scale coal-fired power stations and a heavy reliance on coal within local industry. Because the specific energy efficiency of many industries is low, emissions of aerosols per unit of economic output are high.

The Highveld region (Mpumalanga and Gauteng) is the major industrial area in sub-Saharan Africa and this region plays a major role in the production and transport of aerosols. The urban and industrial areas in these provinces are important source emitters of sulphur, carbon, nitrogen and their corresponding oxides. There exists a high incidence of biomass burning, from farms and human settlements, as well as the combustion of coal and other fuels in the region. This combustion is used to fire the electric power and petrol-chemical industries (the processes of converting coal into synthetic fuels) for the domestic market and for export to other Southern African Development Community countries. These industries are the main source of anthropogenic aerosols (Andreae, 1996; Piketh *et al.*, 1999).

An attempt will be made in this dissertation to evaluate the spatial and temporal variations of atmospheric aerosol loadings over the Highveld, using a ground-based CIMEL sun photometer and handheld hazemeters.

Literature review

Aerosols

Aerosols play an important role in global climate change. They affect the Earth's radiative budget by scattering or absorbing radiation and by altering cloud properties. As a result of their short atmospheric lifetimes (days to weeks), tropospheric aerosols are highly variable in space and time. Quantification of both the direct and indirect effect of aerosols on climate change requires an understanding of the spatial distribution of aerosols, their chemical composition, size distribution, optical and

cloud nucleating properties and suitable models of radiative transfer and cloud physics (Ogren, 1995). This understanding necessitates diverse *in situ* observations (ground-based sensors) and remote-sensing observations (satellites), of aerosol particles on a wide range of spatial and temporal scales. Significant progress has been made in better characterising the direct radiative roles of the different types of aerosols (IPCC, 2001).

Radiation models have been used to estimate the direct radiative forcing for five distinct aerosol species of anthropogenic origin. The global annual mean radiative forcing is estimated as -0.4 Wm^{-2} for sulphate aerosols; -0.2 Wm^{-2} for biomass-burning aerosols; -0.1 Wm^{-2} for fossil fuel organic carbon aerosols; $+0.2 \text{ Wm}^{-2}$ for fossil fuel black carbon aerosols, and in the range of -0.6 to $+0.4 \text{ Wm}^{-2}$ for mineral dust aerosols (IPCC, 2001). The magnitude of these effects, however, is not clearly understood, since there is limited knowledge of the processes that control the distributions as well as the physical, chemical, and optical properties of anthropogenic aerosols. Aerosol radiative forcing remains one of the largest sources of uncertainty in climate change assessment (Houghton *et al.*, 1995).

Aerosol particles may be solid or liquid. They range from $0.01 \mu\text{m}$ to several tens of microns in size. For example, cigarette smoke particles are in the middle of this size range (0.01 to $1^{10} \mu\text{m}$) and typical cloud droplets are $\geq 10 \mu\text{m}$ in diameter. Under normal circumstances, the majority of aerosols form a thin haze in the lower atmosphere (troposphere), from where they fall or are washed out of the atmosphere (by rain) within a period of one week (Herring, 2002).

However, aerosols are also found in the part of the atmosphere just above the troposphere (the stratosphere). Monitoring atmospheric aerosols is difficult. Firstly, in comparison with atmospheric gases, aerosols are highly inhomogeneous and variable. In consequence, aerosol observations have to be both global and continuous in scope. Secondly, the available accuracy of aerosol characterisation is often not sufficient to

ascertain whether indeed aerosols are responsible for climate cooling (Dubovik *et al.*, 2002). For instance, *in situ* measurements, traditionally considered the most reliable observations, are inappropriate for the global monitoring of aerosol radiative forcing parameters and usually do not characterise the aerosol within the total atmospheric column (Sokolik *et al.*, 1993; Sokolik and Toon, 1996).

Since 1980, aerosol distributions and properties have been measured by many space- and ground-based monitoring programmes and intensive field campaigns. While field measurements offer detailed observations of aerosol composition and properties, they are usually limited in spatial or temporal coverage. By contrast, satellite observations provide extensive spatial and temporal coverage, but are short on measurable quantities (such as vertical profiles and aerosol compositions) (Chin *et al.*, 2002). Neither field measurements nor satellite observations alone are sufficient to fully describe aerosol distributions and their physical, chemical, and optical properties. The use of global models, therefore, becomes critical in integrating the satellite and *in situ* measurements. Such models also have to be evaluated by observations before a degree of confidence can be placed in their ability to reflect reality (Chin *et al.*, 2002).

It has been widely documented that high AOT is derived mainly from Aeolian dust and mostly industrially produced sulphur aerosols (Piketh *et al.*, 1999). To further support this assertion, pollution trends have been analysed for the Highveld region for various periods. Earlier analyses showed general increases in pollutants, especially SO₂ levels from coal-fired industries, for the Mpumalanga [formerly Eastern Transvaal] Highveld region and decreases in the Vaal region between 1983 to 1988 (Turner, 1990). He related this to the overall increase in electricity generated by coal-fired power stations over the same period. Trend analysis of SO₂ pollution levels from 1984 to 1995 showed significantly decreasing trends in the central Highveld (at Elandsfontein) and the Vaal Triangle (at Makalu). Significantly, positive trends were observed at the northern Highveld escarpment (at Palmer) and no significant trend

variation was observed over the southern Highveld (at Verkykkop) (Rorich and Galpin, 1998). Relative particulate emissions (kg ash emitted per kWh sent out) have been reduced considerably, through efficient control measures (like bag filters) which have been installed at the majority of power stations, and the implementation of more stringent maintenance and operational procedures within these same stations (Rorich and Galpin, 1998).

This research project focuses on field measurements of aerosol loading over the Highveld region of South Africa.

Sun photometer and hazemeter measurements of aerosol optical thickness at various sampling sites

CIMEL sun-photometer measurements of AOT over Inhaca Island, Mozambique, were carried out between April and November 2000 (Queface *et al.*, 2003). The AOT at Inhaca Island showed day-to-day variability in aerosol loading over a period of 195 days (with ~50 % of total measurements >0.2) which indicated high turbidity in the atmosphere at this location. The levels of AOT (overall mean 0.26) observed at Inhaca are characteristic of a polluted marine atmosphere (based on a mean AOT of 0.07 to 0.08 in a clean marine environment). A seasonal variation in monthly average AOT was observed over Inhaca Island, with an increase in aerosol loading during August to October. This suggested a strong contribution of emissions from biomass burning to the aerosol loading, since August to October is the prime biomass-burning season in southern Africa. Furthermore, the Ångström exponent over Inhaca Island ranged from 0.2 to 2, demonstrating that the tropospheric aerosol loading had several contributing sources. For 70 % of the observations over the island, the Ångström exponent was >1 , showing that fine-mode aerosols dominated atmospheric turbidity at this site. Impacts of fine-mode aerosols over Inhaca Island occur throughout the year. From April to June the aerosol source is not biomass burning but related to either the urban complex of Maputo or to the long-range transport of industrial emissions from the South African Highveld (Queface *et al.*, 2003).

The Southern African Regional Science Initiative 2000 (SAFARI 2000) was a regional project investigating emissions, transport, transformation and deposition of trace gases and aerosols over Southern Africa (Eck *et al.*, 2003). Measurements of the column integrated aerosol optical properties in the region were made by the Aerosol Robotic Network (AERONET) sun-sky radiometers at several sites in August-September 2000, during the dry season. Fine-mode biomass-burning aerosols dominated in the northern part of the study area (Zambia), which is an active biomass-burning region. Other aerosols (including fossil-fuel burning, industrial, and Aeolian coarse-mode types) also contributed to the aerosol mixture in other South African regions. These regions were not as strongly dominated by local biomass burning (Eck *et al.*, 2003). The large amounts of smoke produced in the northern regions led to a north-south gradient in AOT in September, with the biomass-burning aerosol concentrations reduced by dispersion and deposition during transport between August and September (Eck *et al.*, 2003).

Spectral daytime AOT was measured at Sutherland, South Africa (32° 22' S, 20° 48' E) from January 1998 to November 1999. Sutherland is located in the semi-arid Karoo desert, approximately 400 km northeast from Cape Town (Formenti *et al.*, 2002). The same authors noted that the 1998 and 1999 annual average daytime AOT at 500 nm was 0.04 ± 0.04 and 0.06 ± 0.06 , respectively. This seasonal variation was thought to be linked to the biomass-burning season in the southern hemisphere in general and in southern Africa in particular. Smoke haze layers transported to Sutherland originated primarily over the African landmass, at latitudes between 10° and 20° S, and passed over Namibia and Angola. The spectral dependence of the AOT for the smoke layers supports the bimodality of the volume size distribution for aerosols from biomass burning. The accumulation mode had a volume modal diameter of 0.32 μm , consistent with the hypothesis of aged haze (Formenti *et al.*, 2002).

Piketh *et al.* (1999) observed that Aeolian dust and industrially derived sulphur aerosols are the major summer and winter constituents of the ubiquitous southern African haze layer south of 20° S. Industrial emissions from the South African industrialised Highveld are exported out of the region and have an impact on remote regions of the sub-continent (Freiman and Piketh, 2003). This impact has been generated through direct and recirculated transport. Long-range atmospheric transport and recirculation of anthropogenic aerosols and trace gases over southern Africa are expected to impact the radiative balance, photochemistry, and biogeochemistry of the region as a whole.

Effects of anthropogenic aerosols

Aerosol particles are substances emitted either from natural processes or from human activities. The effect of anthropogenic aerosols on the planetary albedo can delay or compensate for carbon dioxide-induced greenhouse warming. In fact, this effect is suspected of causing the slow down in the increase in the global temperatures, decreasing the diurnal temperature ranges, and decreasing the relative differences between warming in the northern hemisphere and the southern hemisphere, and decreasing the warming of the continents relative to the oceans (NASA, 2002). A further consequence of air pollution is loss of visibility. This is primarily due to suspended airborne particles, which scatter light efficiently, giving the atmosphere a “hazy” appearance.

Atmospheric aerosols modify climate conditions by direct absorption and scattering of solar energy, and by secondary means, by fine-mode aerosols acting as auxiliary cloud condensation nuclei, thereby decreasing average cloud droplet size and enhancing planetary albedo (Charlson and Heintzenberg, 1995; Charlson, 1997; Facchini *et al.*, 1999).

In addition, absorbing aerosols may also modify climate by the semi-direct effect (Hansen *et al.*, 1997) whereby the heating of the aerosol layer reduces cloud cover by

either increasing atmospheric stability or by evaporating clouds (Ackerman *et al.*, 2000).

South Africa, and especially its industrial Highveld, is a major source of anthropogenic and natural aerosols and trace gases in the southern sub-continent. This region produces >1 Mt of SO₂ a year, mainly from the burning of coal (Terblanche *et al.*, 2000). The high particle concentration in the atmosphere of Soweto, and other similar high-density residential areas, remains one of the most serious air-quality problems in South Africa. Heavy blankets of black smoke are characteristic of the winter atmosphere over Soweto, a large conurbation southwest of Johannesburg (Wentzel *et al.*, 1999). Photochemical haze is an increasing phenomenon in larger cities (such as Johannesburg and Pretoria), with vehicle emissions considered to be the major contributor (Annegarn, 1997). The brown haze prevalent in Cape Town is also attributed to vehicle emissions (de Villiers *et al.*, 1997). Other activities, such as veld burning and biogenic emissions, are among the larger contributors to the regional haze.

South African atmospheric conditions

Southern Africa is situated geographically beneath the planetary-scale, southern hemisphere descending limb of the Hadley circulation throughout much of the year. This atmospheric circulation is characterised by the regular occurrence of semi-permanent, subtropical anticyclones. Subsidence predominates in the high-pressure cells – which occur on average nearly 50 % of the days of the year over South Africa – and reaches a maximum frequency of around 80 % during the austral winter (Tyson *et al.*, 1996). The high frequency of occurrence of subsiding atmospheric circulation regimes leads to the distinctive lamination of the troposphere in which absolutely stable layers occur.

Four absolutely stable layers may be identified in the troposphere over southern Africa. The two lowest layers appear to be of greatest significance in controlling both

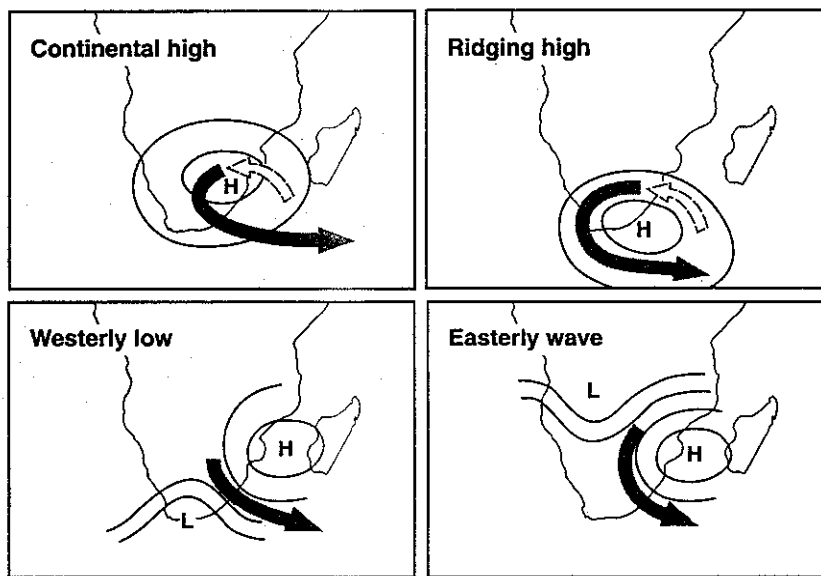
horizontal and vertical transport, since they occur with high frequency and spatial ambiguity. The lowest discontinuity is usually associated with the top of the daytime mixing layer, occurring at ~1500 m above the interior plateau surface (at an altitude of approximately 3000 m above sea level (ASL)). This inversion is broken every 5 to 7 days by the passage of westerly disturbances, allowing the convective mixing of aerosols and trace gases to greater heights (Garstang *et al.*, 1996; Cosijn and Tyson, 1996; Swap and Tyson, 1999).

The effects of aerosol accumulation are evident to the naked eye at the ~700 hPa and ~500 hPa levels over the interior of South Africa, particularly in winter. On days when the absolutely stable layers are observed, dense dust and haze belts are also present at these two levels as a major discontinuity between the hazy, polluted lower tropospheric air and clear air aloft (Tyson *et al.*, 1996).

The atmosphere is constantly in motion and circulates on a variety of scales, ranging from the local and mesoscale to the synoptic and larger macroscale. Any aerosols or trace gases suspended within the atmosphere, particularly those near the land surface, will be transported on the same scales by the air in circulation (Tyson and Preston-Whyte, 2000). Transport of aerosols and trace gases in the troposphere over southern Africa and the adjacent ocean areas is driven by the interacting planetary and synoptic scale features of the general circulation of the southern hemisphere. The semi-permanent south Atlantic anticyclone, the continental anticyclone over southern Africa, and the south Indian anticyclone have a dominant effect on all regional transport patterns. The location of the downward limbs of the Walker Circulation, the position of the semi-stationary easterly waves over the sub-continent, and the changing westerly wave structure in the mid-latitudes to the south also play an important role (Garstang *et al.*, 1996).

Synoptic scale atmospheric transport over southern Africa

With most of the different types of synoptic circulation fields that occur in the lowest layers of the atmosphere over southern Africa, the transport of air and whatever is carried within it, is predominantly towards the east coast and the Indian Ocean (Tyson and Preston-Whyte, 2000) (Figure 1.1).



Source: Tyson and Preston-Whyte, 2000:289

Figure 1.1: The main transport pathways associated with different circulation types over southern Africa

During the process of recirculation over southern Africa, air sandwiched between the different stable layers may become decoupled from that circulating in the layers above and below. Even though aerosols have a short residence time in the atmosphere, depending on their particle size and the prevailing atmospheric conditions, they are transported over great distances by air masses. Vertical transport is controlled by the stability structure of the atmosphere and horizontal transport by the local thermo-topographic winds near the land surface or by large-scale circulation

in changing synoptic flow fields (Tyson and Preston-Whyte, 2000). The dominant atmospheric circulation patterns and air transport climatology over South Africa have been well documented by Tyson *et al.* (1996). The variations in the spatial and temporal concentrations of aerosols have been shown to be associated with different air mass transport pathways over South Africa (Garstang *et al.*, 1996; Tyson *et al.*, 1996; Tyson., 1999).

Four main circulation types (semi-permanent subtropical anticyclones, transient mid-latitude ridging anticyclones, westerly baroclinic disturbances, and barotropic quasi-stationary tropical easterly waves) dominate atmospheric circulation over southern Africa, with varying frequencies throughout the year, and the four types are associated with different air mass transport pathways (Tyson *et al.*, 1996).

Aerosols and their potential for climate forcing have been discussed. The Highveld region of South Africa plays a substantial role in the production and transport of aerosols. This is due to the large urban and industrial areas that abound in the region. A detailed examination will be undertaken of the spatial and temporal distribution of aerosol loading over the Highveld region.

CHAPTER 2:

DATA AND METHODOLOGY

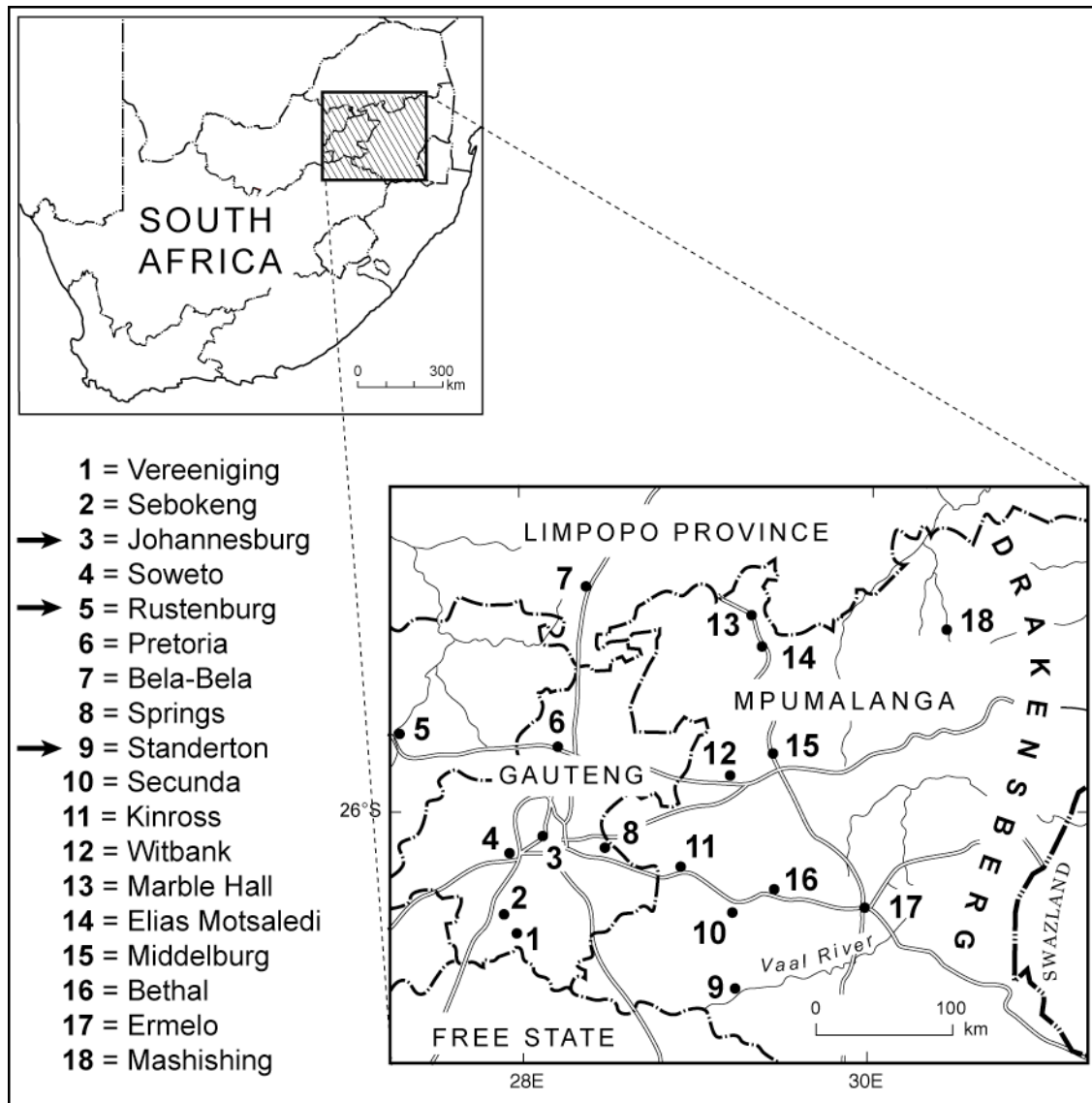
The methodology for investigating the spatial and temporal distribution of aerosol loading over the Highveld region is outlined. The location of the sample areas is provided. The hazemeter used for the data collection, its parameters and how it functions, is described. An explanation of how the data was processed is also presented.

Highveld site description

The Highveld is an elevated plateau, between 1200 m and 1700 m ASL. This region receives annual rainfall between November and April. The plateau is the source area for many of South Africa's major rivers, including the Vaal and the Orange rivers. It is an important agricultural area and the abundance of gold, coal and other minerals has led to the development of this region as the centre of the South African industrial sector (Terblanche *et al.*, 2000).

The sites considered in the study (Figure 2.1) range in altitude from 914 m to 1724 m ASL. Fifteen (15) (in 2002) and eighteen (18) (in 2003) hand-held hazemeters (used to measure AOT) were dispatched to the areas chosen for the sampling periods. Details of each site are given in Table 2.1. Three areas indicated (with arrows in Figure 2.1) were used only in winter 2003. In 2003 the eighteen (18) areas were chosen to coincide with regional sources and/or the likely paths of known transport of aerosols over the Highveld region. Hazemeters were used not only to investigate aerosol loading over the region but also to ascertain which areas were prone to elevated levels of aerosols because of their relative location to industry or built-up areas (including townships). The sites were divided into three (3) main categories,

based on the activities taking place (township, industrial/urban and agricultural), in order to better understand the variations in the levels of aerosol loading.



The arrows indicate sites used in winter 2003 only

Figure 2.1: Location of hazemeters over the Highveld region during 2002 and 2003

Table 2.1: Location and classification of hazemeter sites over the Highveld region

School	Site location	Site classification	Latitude and Longitude	Altitude (m ASL)
Maope Secondary School †	Bela-Bela	A	24° 53' S 28° 16' E	1146
Rockcorner Combined School	Elias Motsaledi	A	25° 10' S 29° 23' E	953
Excelsior College	Marble Hall	A	24° 59' S 29° 17' E	914
Boikgagong Secondary School *	Rustenburg	I/U	25° 37' S 27° 16' E	1122
Parktown Girls' High School *	Johannesburg	I/U	26° 12' S 28° 02' E	1643
Eastdene Combined School	Middelburg	I/U	25° 45' S 29° 27' E	1487
Pretoria Girls' High School #	Pretoria	I/U	25° 45' S 28° 13' E	1373
Highveld Park High School	Secunda	I/U	26° 30' S 29° 12' E	1640
Springs Boys' High School	Springs	I/U	26° 15' S 28° 25' E	1600
Riverside High School	Vereeniging	I/U	26° 40' S 27° 57' E	1486
Thomas Percy Sililo School	Witbank	I/U	25° 55' S 29° 14' E	1669
Ziketheleni Secondary School *	Standerton-	T	25° 51' S 29° 13' E	1603
Ihkhethelo Secondary School	Bethal	T	26° 26' S 29° 27' E	1652
Cebisa Secondary School	Ermelo	T	26° 31' S 29° 59' E	1724
Thistle Grove Combined School	Kinross	T	26° 25' S 29° 05' E	1673
Mashishing Secondary School +	Mashishing	T	25° 08' S 30° 24' E	1476
Boikgathelo Secondary School	Sebokeng	T	26° 29' S 27° 50' E	1552
Diepdale Secondary School †	Soweto	T	26° 14' S 27° 56' E	1137
† Winter 2002 and summer 2002 data discarded as learners did not collect data on the days specified, the sky was cloudy and/or the instruments were faulty. * Site used in 2003 only. # Winter 2002 data collected for only 11 days as hazemeter malfunctioned for 21 days of this				

sampling period.

- + Data collected in summer 2002 and winter 2003 only because a site in the Mashishing area was established ahead of summer 2002 owing to faulty hazemeters.

A Agricultural
I/U Industrial/urban
T Township

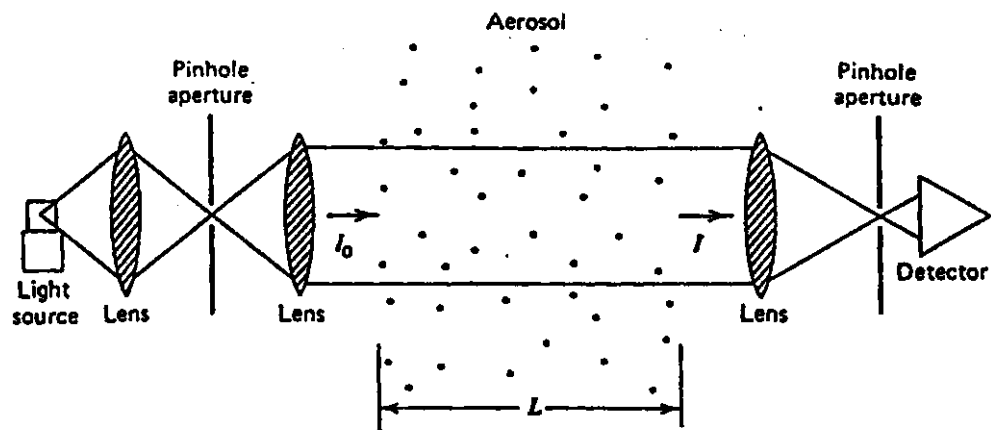
The Highveld haze project involved secondary schools, whose Grades 10 and 11 learners were introduced to the instrumentation and how it works (Figure 2.2). The learner involvement was done in conjunction with the Physical Science curriculum component on the electromagnetic spectrum. The learners were also introduced to some of the analysed data, specifically on how it related to the general pattern of air pollution in their respective regions.



Figure 2.2: Grade 10 and 11 learners using a hazemeter during the launch of the Highveld haze project

Data collection

Extinction of radiation can be measured by observing the intensity, I , of a light source as seen through a volumetric object with scattering particles, where I_0 is the intensity of the same light source seen through the same volume without scattering particles. This method can be applied in the atmosphere to measure the attenuation of solar radiation by aerosols (Iqbal, 1983). Sun photometers and hazemeters use this principle of operation. The lenses on both types of instrument can be prepared to allow certain wavelength ranges of solar radiation energy to pass through them (Figure 2.3), thereby measuring the level of solar radiation at different wavelengths. Once the AOT has been computed, the size of the particles can then be evaluated using the Ångström exponent formula.



(Source: Bohren and Huffman, 1983:56)

Figure 2.3: Schematic diagram of an extinction measuring apparatus

CIMEL sun photometer

The CIMEL sun photometer has been designed to measure sun and sky radiance in order to derive total column water vapour, ozone and aerosol properties, using a combination of spectral filters and azimuth/zenith viewing controlled by a microprocessor (Schafer *et al.*, 2002). The instrument (Figure 2.4) is equipped with a narrow band-pass filter in the visible and near infrared wavelengths with centre wavelengths of 440, 670, 870, 936, 940 and 1020 nm. The CIMEL sun photometer provides the AOT at each of these wavelengths (except for the 940 channel, which is used to derive total column water vapour). In addition to the direct solar irradiance measurements that are made with a field view of 1.2°, the instrument measures the sky radiance in four spectral bands (440, 670, 870, and 1020 nm) along the solar principal plane up to six times a day (Schafer *et al.*, 2002).

The instrument takes a pre-programmed sequence of measurements between 07:00 and 19:00 local time. Data products are the spectral AOT (nominal error of ± 0.01), the aerosol column volume distribution, the spectral complex refractive index, the asymmetry parameter, and the single scattering albedo (Dubovik *et al.*, 2002; Holben *et al.*, 2001). The CIMEL sun photometer, as a reference point for the hazemeters located at the sampling sites, was situated at S26°20' E28°13' at an altitude of 1775 m ASL (at the University of the Witwatersrand, Johannesburg). This instrument was used to calibrate the hazemeters at 440, 670, 870, and 1020 nm sky radiance for the duration of the study.



Figure 2.4: The CIMEL sun photometer situated at the University of the Witwatersrand

The hazemeter

The hazemeter (Figure 2.5) can collect and store data information for more than 120 days. The data are measured in six analogue channels: four bands measure solar intensity, while temperature and battery voltage are measured by the remaining two channels (Brooks and Mims, 2001). A combination of light-emitting diodes and a phototransistor are used to sense solar energy received at nominal wavelengths of 380, 530, 680, and 880 nm (Table 2.2). Solar sensor signals are amplified, buffered and converted by the micro-controller to a unipolar 10-bit digital value (Brooks and Mims, 2001). Readings are taken approximately every 30 min daily, during periods of full sunshine. The hazemeter reads each spectral band approximately 600 times a second to catch the maximum reading (when the instrument is pointed at the sun correctly). Every 32 readings are added and averaged, to define a reading that reduces random noise for each band. Each new average value is compared to the previous high and low values for each spectral band. The maximum value for the red solar sensor is displayed for the current measurement for each spectral band.

When each value displayed no longer increases, the control button is pressed to store the time (the difference between the maximum and minimum average reading that compensates for the minimum or dark reading), and other information (such as the save number in non-volatile memory). This step also powers down the instrument until the next measurement (Brooks and Mims, 2001). When the energy travels through the sun-light view tubes, the light passes through a filter which isolates the particular wavelength to be analysed by the instrument. The hazemeter records a voltage reading for each filter. The voltage is proportional to the strength of the energy determined at a specific wavelength. The AOT can be calculated from these values to determine the type of aerosol present in the atmosphere (Brooks and Mims, 2001). The photodiode filter channels isolate the following wavelengths from direct sunlight: 880 nm (infrared), 650 nm (visible), 500 nm (visible), and 405 nm (visible) (Table 2.2). An RS-232 port transfers several months of readings, collected in the micro-controller data file, to a computer for additional computation. Fifteen (15) hazemeters were used in the different designated sites for the 2002 sampling periods. The same hazemeters plus three (3) additional hazemeters were utilised during the winter 2003 sampling period, although, at NASA's request (Newcomb, 2003: personal communication), all the diodes on the hazemeters were changed prior to the study period to give more accurate AOT readings.

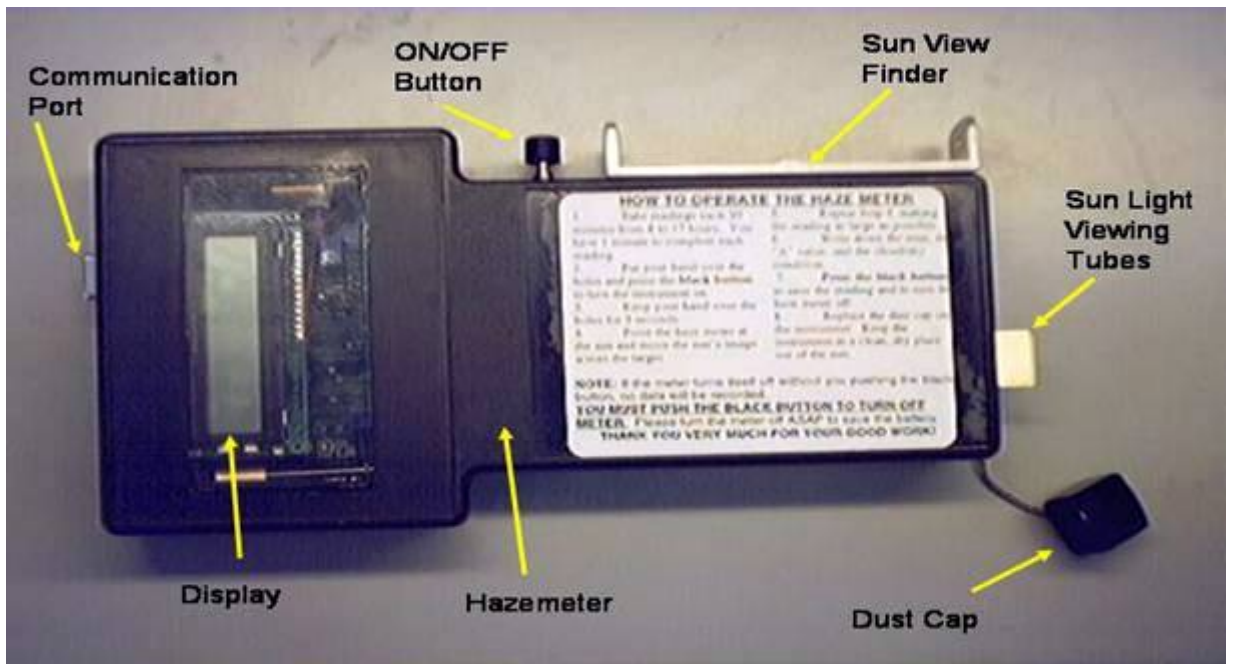


Figure 2.5: A hazemeter used in the research

Table 2.2: Spectral bands used to measure aerosol optical thickness over land

MODIS band (nm)	AERONET band (nm)	Hazemeter band (nm)	Hazemeter bands used during 2002 (nm)	Hazemeter bands used during 2003 (nm)
Not available	870	880 (850 to 905)	880	880
660 (620 to 670)	670	680 (680 to 690)	680	680
550 (545 to 565)	500	530 (510 to 550)	530*	500*
470 (459 to 479)	440	Not available	Not available	Not Available
Not available	380	380 (360 to 410)	380	405
<p>* Hazemeter bands used for data analysis. Source: GLOBE, 2002:17</p>				

Table 2.3 is a tabular representation of typical AOT ranges. “Optical thickness” describes how much light passes through a material. The amount of light transmitted can be quite small (<1 %) or very large (nearly 100 %).

Table 2.3: Typical ranges for aerosol optical thickness

Sky conditions	Channel
Extremely clear	0.03 to 0.05
Clear	0.05 to 0.10
Somewhat hazy	0.10 to 0.25
Hazy	0.25 to 0.5
Extremely hazy	>0.5
<p>Source: GLOBE, 2002:23</p>	

Measurements of AOT were made using hazemeters and a CIMEL sun photometer, during a 32-day winter sampling period (21 May to 21 June) in 2002; during a 32-day summer sampling period (21 October to 21 November) in 2002, and during a 32-day winter sampling period (19 May to 19 June) in 2003. Before the 2003 winter sampling period, the diodes on the hazemeters were changed (at NASA's request – Newcomb, 2003: personal communication) to give more accurate AOT readings. The changes made to hazemeters gave results that were similar for winter and summer sampling periods. This is a very unlikely scenario.

During the sampling periods, data were collected daily from 07:00 to 17:00 local time at 30 min intervals. Instruments were distributed to 18 different schools, where Grade 10 and 11 learners collected the measurements.

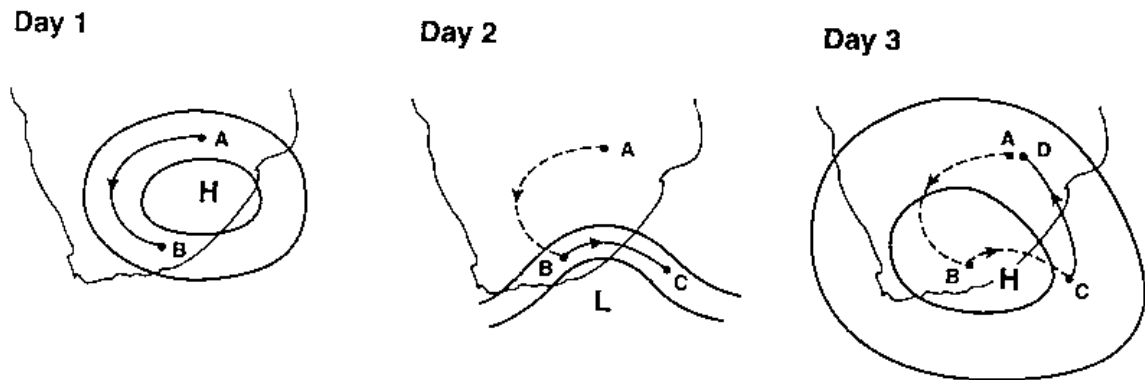
Inter-calibration with the CIMEL sun photometer was undertaken before and after each sampling period. The data downloaded from the hazemeters were sent to the National Aeronautical Space Administration (NASA) for processing.

Data from Bela-Bela and Soweto for both the winter and summer 2002 sampling periods were not of sufficiently high quality and were, therefore, not included (Table 2.1). Mashishing was used as a site in the summer 2002 and winter 2003 sampling periods. The Pretoria site, in the winter 2002 sampling period, had data collected for a period of only 11 days (the hazemeter malfunctioned on 21 days during that time).

Trajectory analysis

The HYSPLIT_4 (Hybrid Single-Particle Lagrangian Integrated Trajectory) trajectory model output, generated on-line by the National Oceanic and Atmospheric Administration (NOAA) Air Resources Laboratory was employed for trajectory analysis. Trajectories are paths followed by air parcels with time. They provide a useful tool for understanding the three-dimensional transport of airborne material in

the atmosphere as shown in the analysis in Chapter 3 (Draxler and Hess, 1998). The horizontal transport of air and what is contained therein may be determined by trajectory analysis. The principle of trajectory analysis is demonstrated in Figure 2.6.



Source: Tyson and Preston-Whyte 2000: 285

Figure 2.6: Three-day transport of atmospheric particulates with different circulation systems over South Africa

According to Tyson and Preston-Whyte (2000), on day 1 aerosols are transported from A to B along trajectory AB. By the time the aerosols arrive at point B, the pressure pattern and its associated circulation have changed from anticyclonic to cyclonic. So, on day 2, transport continues along trajectory BC, to give the two-day trajectory ABC. By the time the aerosols reach point C, the synoptic situation has become affected by a ridging anticyclone and the material continues along a new trajectory CD. This gives a complete three-day trajectory ABCD.

In this research, backward trajectories were calculated using a 7-day period and 24-hour run time for the three sampling periods. Air parcel trajectories were computed at 14:00 (12:00 GMT) at 850 hPa, 700 hPa and 500 hPa levels.

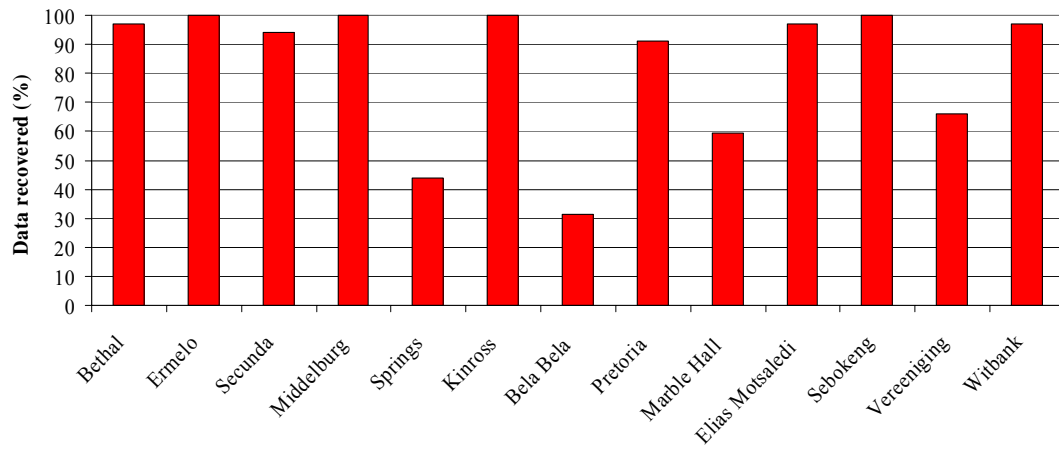
Statistical analysis

Statistical analysis was performed in order to determine the frequency of occurrences of AOT at different channels. The same procedure was undertaken to calculate the Ångström exponent at all the sites studied. The analysis was undertaken to determine the most frequently occurring range in AOT and Ångström exponents, specifically to establish the turbidity over the sampling sites. This analysis was also used to gauge the predominant aerosol size range, as seen from the Ångström exponent. The statistical analysis was performed using the data analysis tool-pack in the EXCEL 2003 and QUATTRO PRO 9 spreadsheets.

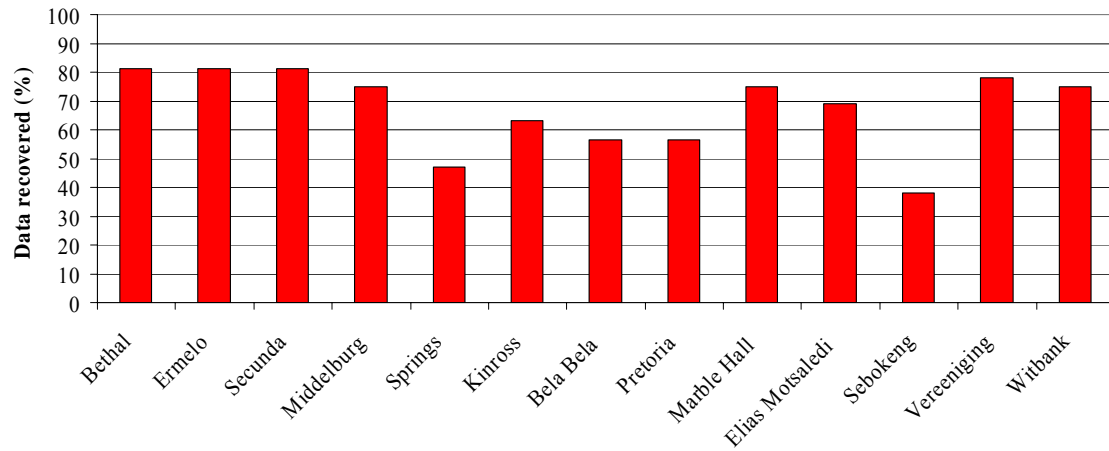
Data recovery

Data collected as a percentage for the entire sampling period are given in Figure 2.7. Overall, the data recovery process was satisfactory (Table 2.1). Data collection was dependant on weather conditions since cloud-free conditions are needed. Summer is traditionally the rainy season on the Highveld and this, ultimately, eliminated periods of overcast or rainy weather from the data collection.

a)



b)



c)

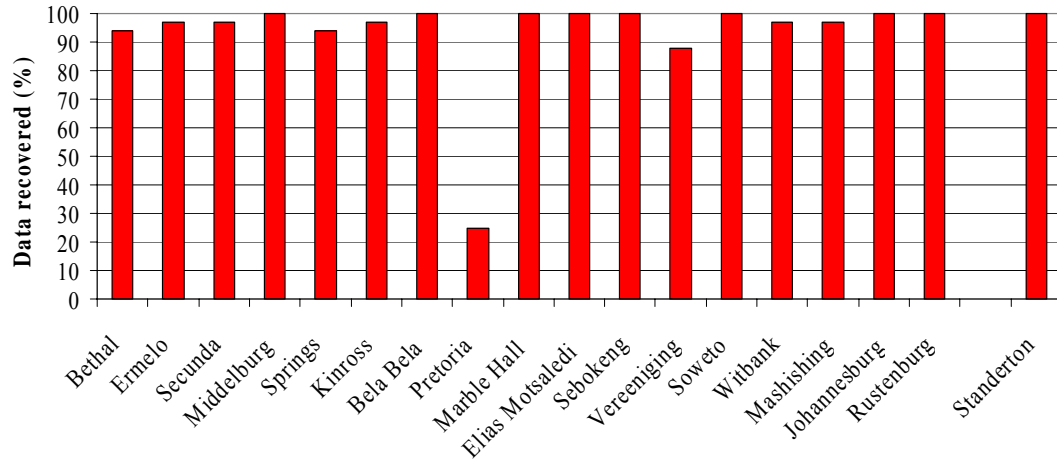


Figure 2.7: Data collected as a percentage during a) winter 2002, b) winter 2003 and c) summer 2002

Surface synoptic charts

Surface synoptic charts are produced daily by the South African Weather Service and were used as a visual aid to determine the reasons for changes in aerosol loadings not clearly evident in the trajectory analysis.

The methodology used to collect and analyse the data obtained from the sun photometer and the hazemeter has been discussed. The use of trajectory analysis, statistical analyses and surface synoptic charts has also been outlined.

CHAPTER 3: DISTRIBUTION OF AEROSOLS OVER THE HIGHVELD

The seasonal variation of aerosol optical thickness and the factors accounting for these changes over the South African Highveld will be considered in this chapter. Aerosol size and the dependence of water vapour content will also be discussed.

Seasonal variation of AOT over the Highveld

AOT measured over the Highveld by hand-held hazemeters was shown to vary between 0.05 and 1 during the three sampling periods (Figure 3.1). Measurements during the summer 2002 sampling period showed an increase in the average AOT_{530nm} . This was an unexpected finding since the AOT_{530nm} is generally expected to be higher during winter months (Swap and Tyson, 1999). During winter, aerosols accumulate in the atmosphere because of absolutely stable layer conditions. The highest AOT_{530nm} (that is, 1) was measured during the winter 2002 sampling period. The distribution of AOT values for three sampling periods were very similar (Figure 3.1). The only important difference is the notably higher frequency of occurrence of AOT values higher than 0.4 during the summer 2002 ($\pm 14\%$). These periods will be discussed later in this document.

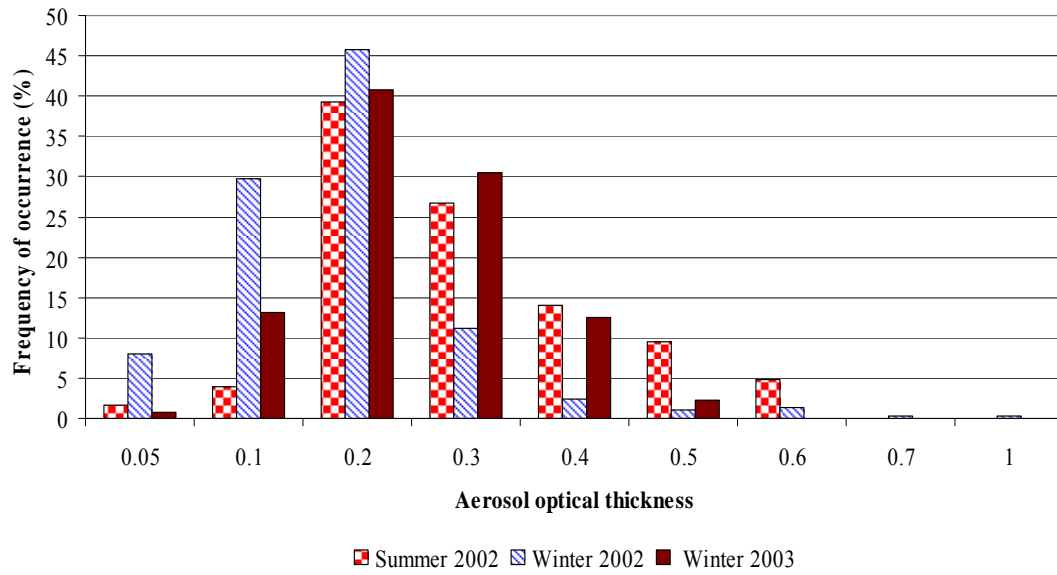


Figure 3.1: Frequency of occurrence of daily aerosol optical thickness during summer 2002 (AOT_{530nm}), winter 2002 (AOT_{530nm}) and winter 2003 (AOT_{500nm}) for all sites over the Highveld region

Variation between township, industrial/urban, and agricultural sites

This variability is also because each site type (township, industrial/urban and agricultural) has different activities that impact the aerosol loads differently at any given time.

Township sites

Seasonal differences were recorded at the Bethal, Sebokeng, Mashishing and Kinross sites, with the highest AOT_{530nm} being recorded during the summer 2002 sampling period. The occurrence of the average daily $AOT_{530nm} > 0.4$ at the sites was only recorded during the 2002 summer sampling period when the AOT_{530nm} in the Highveld townships reached 0.6 and above. During the winter 2002 sampling period, the average daily AOT_{530nm} did not exceed 0.5 (Figure 3.2). The aerosol loading causing higher AOT during the summer 2002 sampling period (Figure 3.3) appeared to be mainly from atmospheric dust (many of the township sites have unvegetated surfaces and a higher percentage of unpaved roads) and , and the burning of refuse, waste and cut grass in the vicinity of the surrounding dwellings. Other sources of aerosol particles were from the burning of coal, particularly early in the morning and late in the evening (Väkeva *et al.*, 1999; Chimidza and Moloji, 2000).

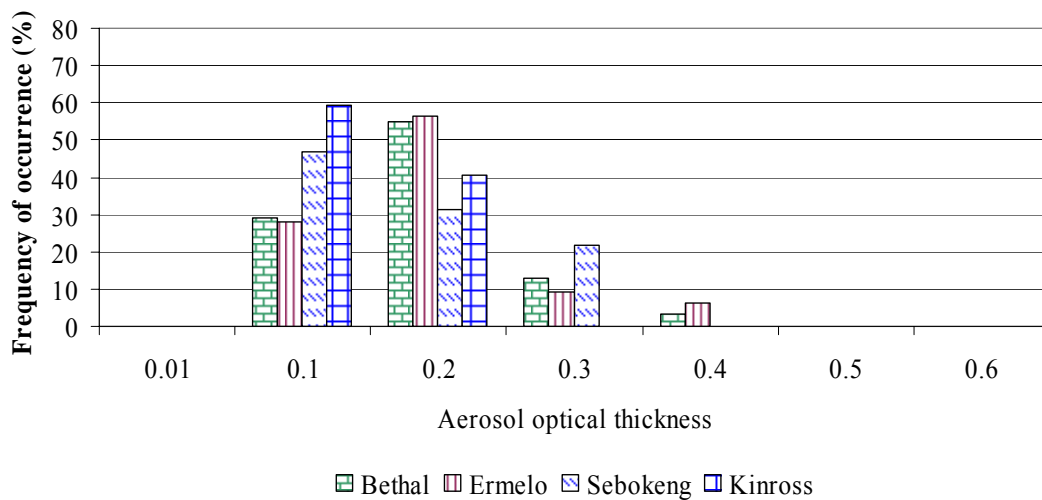


Figure 3.2: Frequency of occurrence of daily average AOT_{530 nm} for township sites during the winter 2002 sampling period

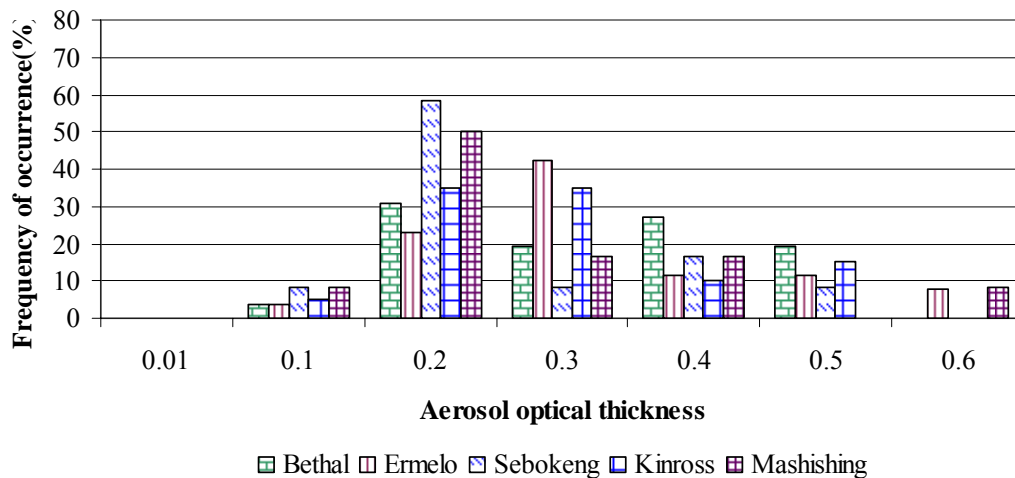


Figure 3.3: Frequency of occurrence of daily average AOT_{530 nm} for township sites during the summer 2002 sampling period

Industrial/urban sites

At almost all industrial/urban sites an AOT_{530nm} of 0.2 was observed most frequently in both the winter and summer 2002 sampling periods. The winter and summer 2002 results (Figure 3.4 and 3.5) for almost all sites also showed episodes of high AOT_{530nm} . The measured high AOT_{530nm} are linked to the high concentration of industrial and vehicular activity at these sites.

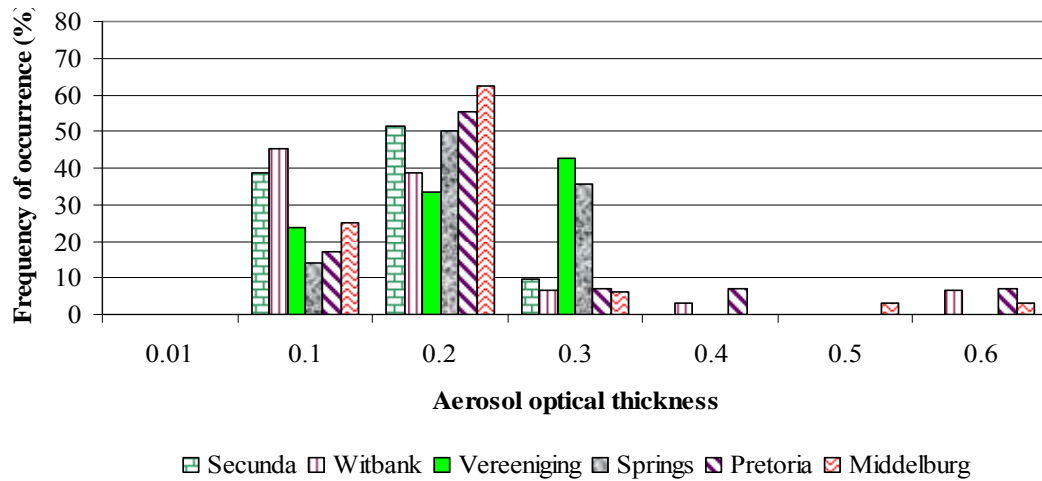


Figure 3.4: Frequency of occurrence of daily AOT_{530nm} for industrial/urban sites during the winter 2002 sampling period

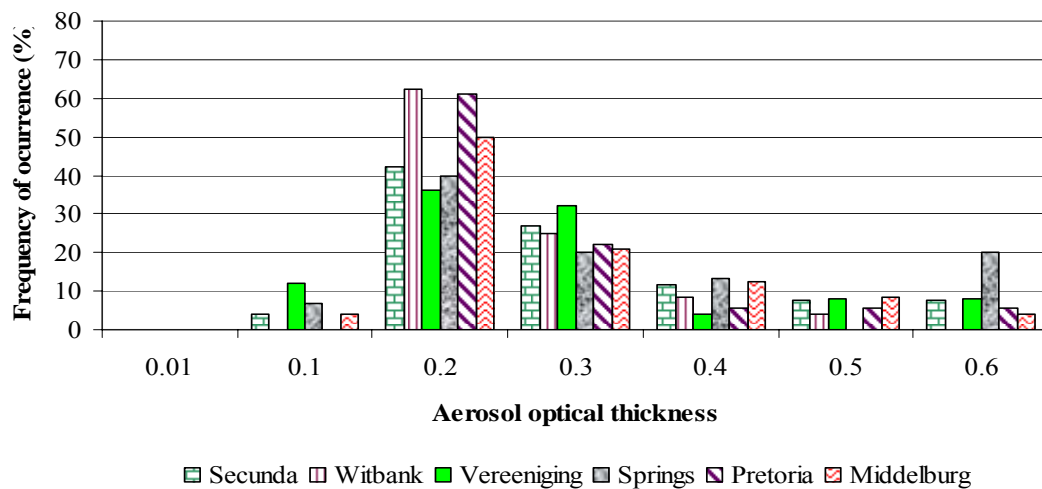


Figure 3.5: Frequency of occurrence of daily AOT_{530nm} for industrial/urban sites during the summer 2002 sampling period

Agricultural sites

An AOT_{530nm} of 0.1 occurred most frequently (up to 80 % of days) at all the agricultural sites during the winter 2002 sampling period (Figure 3.6). Marble Hall had a 42 % occurrence of 0.2 AOT_{530nm} measured in both the winter and summer 2002 sampling periods. This has been attributed to the burning of tyres in the winter 2002 sampling period (to keep pests away) and the tilling of agricultural land (in preparation for the summer rains). During the summer 2002 sampling period, there was variability in the data set of aerosol loading at each site (Figure 3.7a). The AOT numbers during summer are generally higher than during winter (Figure 3.8). But there seems to be a drop in the background values at the end of October. This could be from decreased biomass burning emissions from the North.

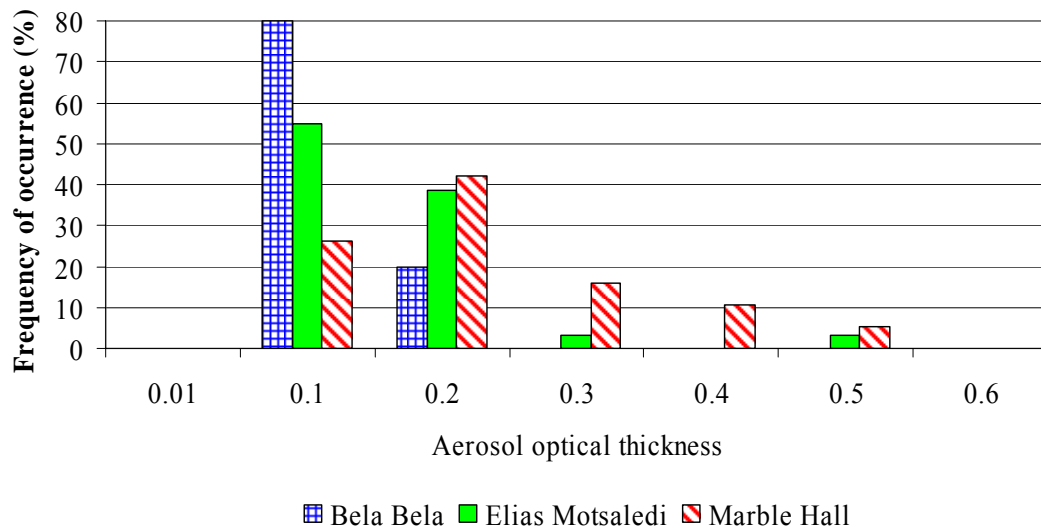


Figure 3.6: Frequency of occurrence of daily AOT_{530nm} for agricultural sites in the winter 2002 sampling period

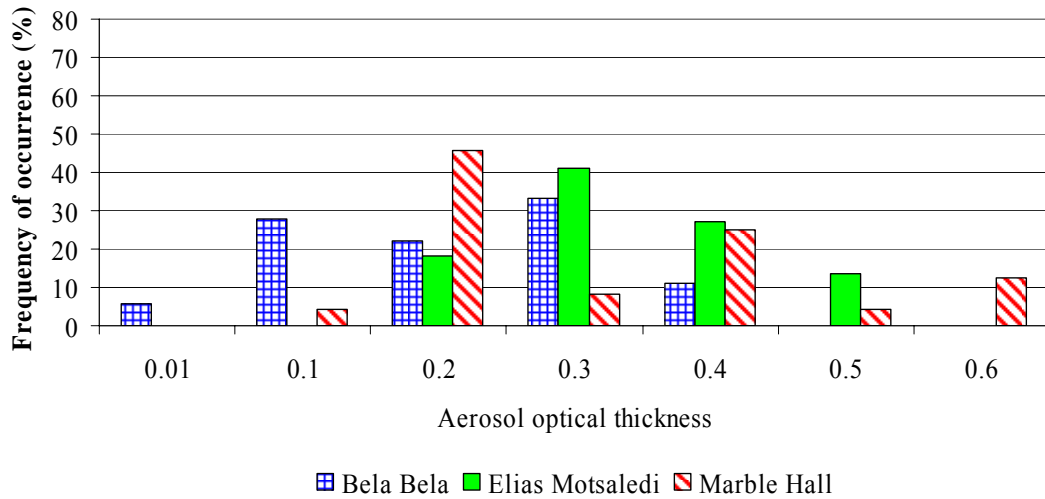


Figure 3.7: Frequency of occurrence of daily AOT_{530nm} for agricultural sites during the summer 2002 sampling period

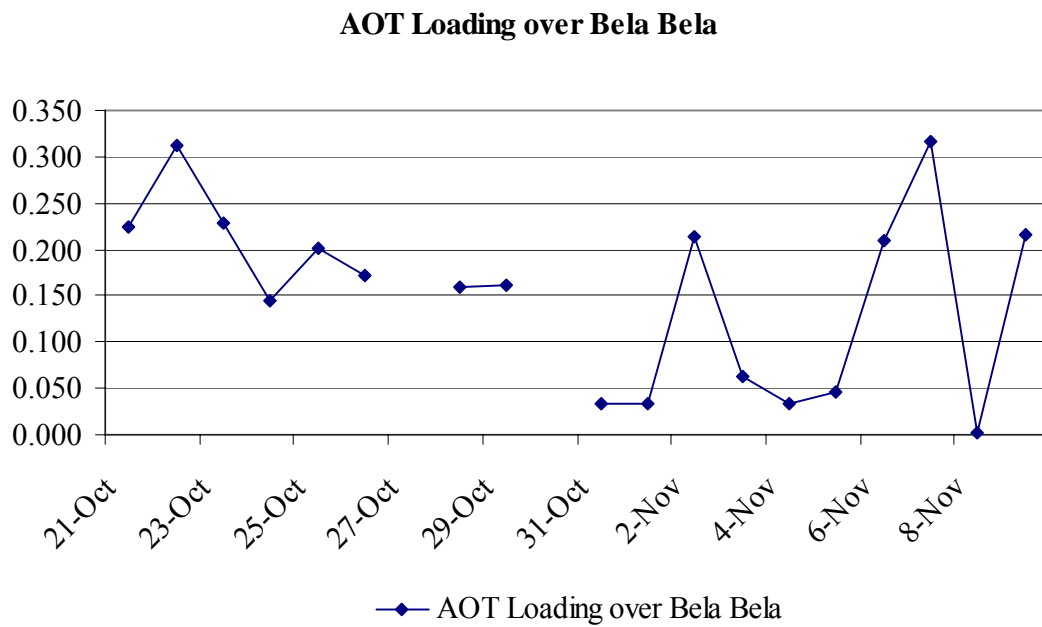


Figure 3.8: Daily AOT_{530nm} for Bela Bela during the summer 2002 sampling period

Wind speed and wind direction during the 2002 sampling periods

Wind speeds recorded during the winter 2002 sampling period (3.8ms^{-1}) (Figure 3.9) were slightly lower than during the summer 2002 sampling period (4.6ms^{-1}) (Figure 3.10). This seems to confirm that indeed biomass burning products were prevalent in winter and predominantly from the North.

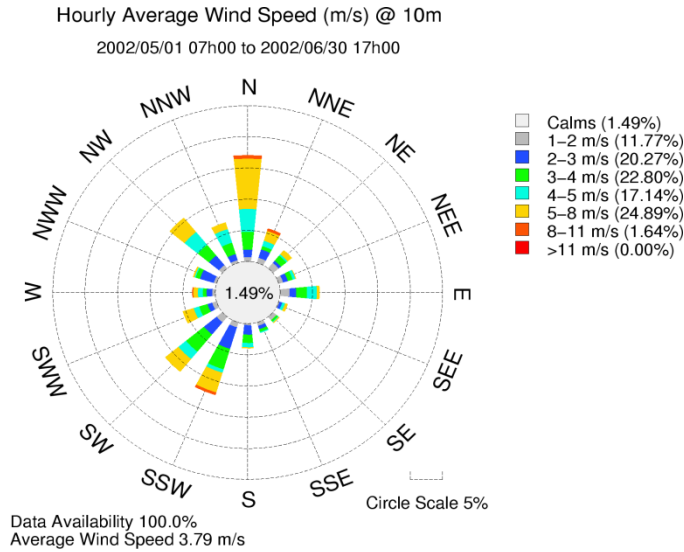


Figure 3.9: Hourly average wind roses depicting the prevailing winds in winter 2002 calculated at the OR Tambo International Airport

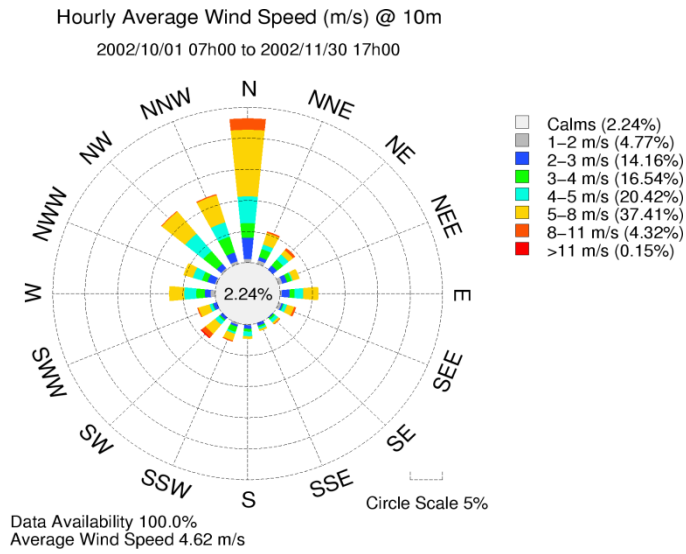


Figure 3.10: Hourly average wind roses depicting the prevailing winds in summer 2002 calculated at the OR Tambo International Airport

Higher AOT_{530nm} at township and agricultural sites in the summer 2002 sampling period may have been due to the higher humidity levels during this time.

Spatial variation in AOT_{530nm} across the Highveld

There is a difference in AOT_{530nm} build-up across the Highveld region between the winter and summer 2002 sampling periods (Figures 3.11 and 3.12). AOT_{530nm} increased across the Highveld from the southwest. This was due to the prevailing winds from the north-northwest in summer. Moist unstable conditions and rainfall are confined almost exclusively to summer months. In the dry winter 2002 sampling period, the AOT_{530nm} was highest over the central Highveld region. In the winter and summer 2002 sampling periods, within agricultural regions, the AOT_{530nm} was constantly high. The highest AOT_{530nm} during the winter 2002 sampling period was not recorded over the main pollution sources but over agricultural sites. During the summer 2002 sampling period, the highest AOT_{530nm} occurred at the same (agricultural) sites, with high loadings directly downwind of the major industrial sources of emissions.

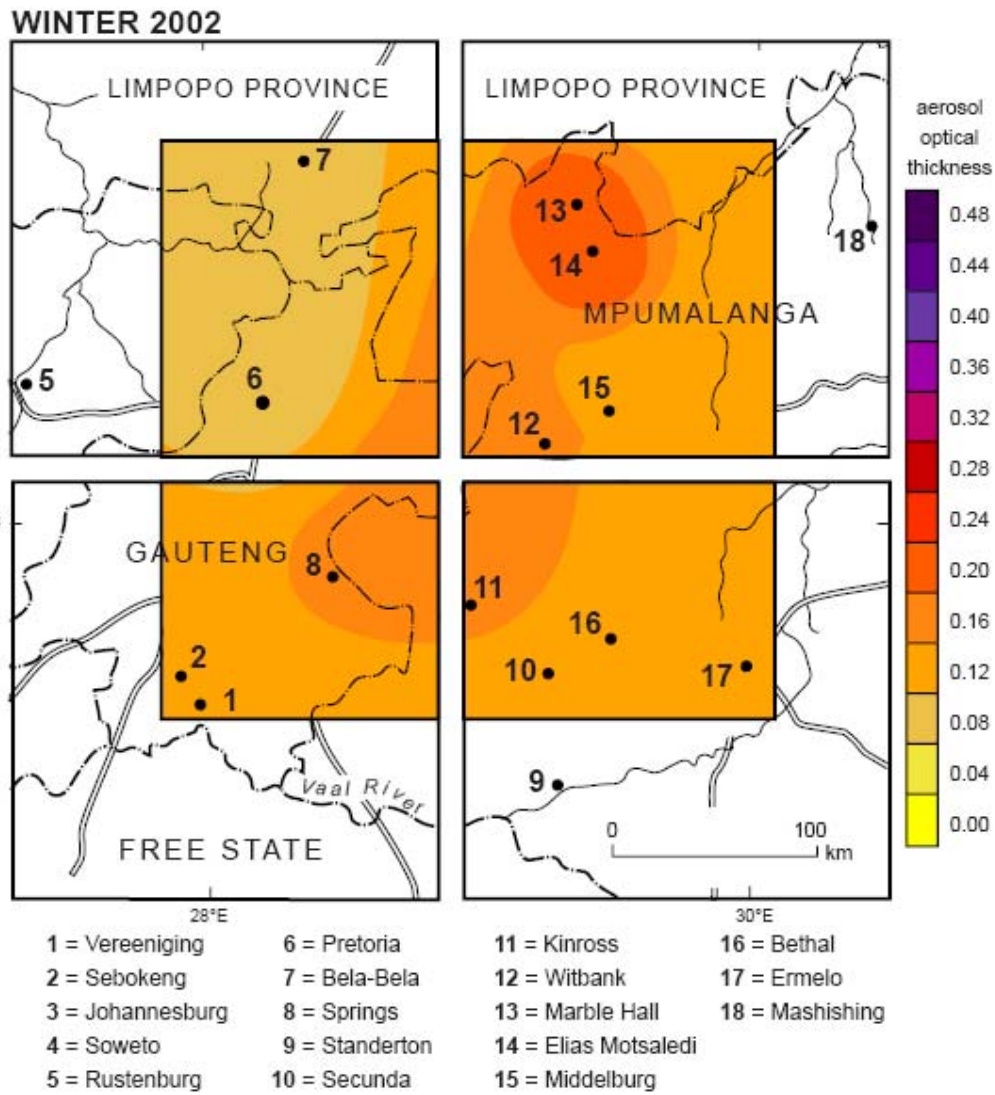


Figure 3.11: Spatial variation of AOT_{530nm} over the Highveld region in winter 2002

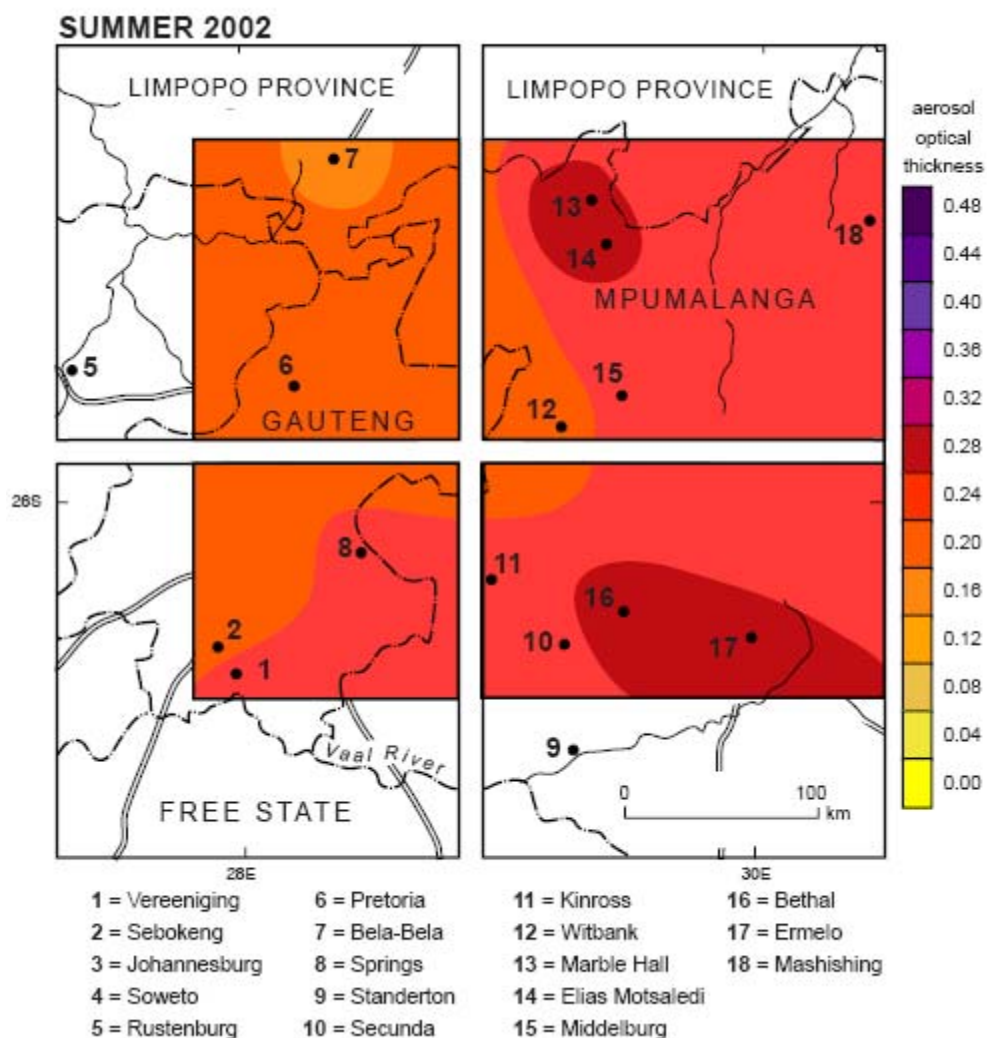


Figure 3.12: Spatial variation of AOT_{530nm} over the Highveld region in summer 2002

Correlation of aerosol optical thickness between sites

Township sites

No correlation was found between any of the township sites during the winter and summer 2002 sampling periods. This was because the AOT_{530nm} was found to be a function of local sources at these sites. Figure 3.13 is a geographical depiction of the relative positions of these sites across the Highveld region. Although no vertical

measurements were performed over these sites, it is postulated that the bulk of the aerosol loading will occur near the surface layer, extending to approximately 1200 m above the surface in winter and slightly higher during summer (Tyson *et al.*, 1996) (Table 3.1).

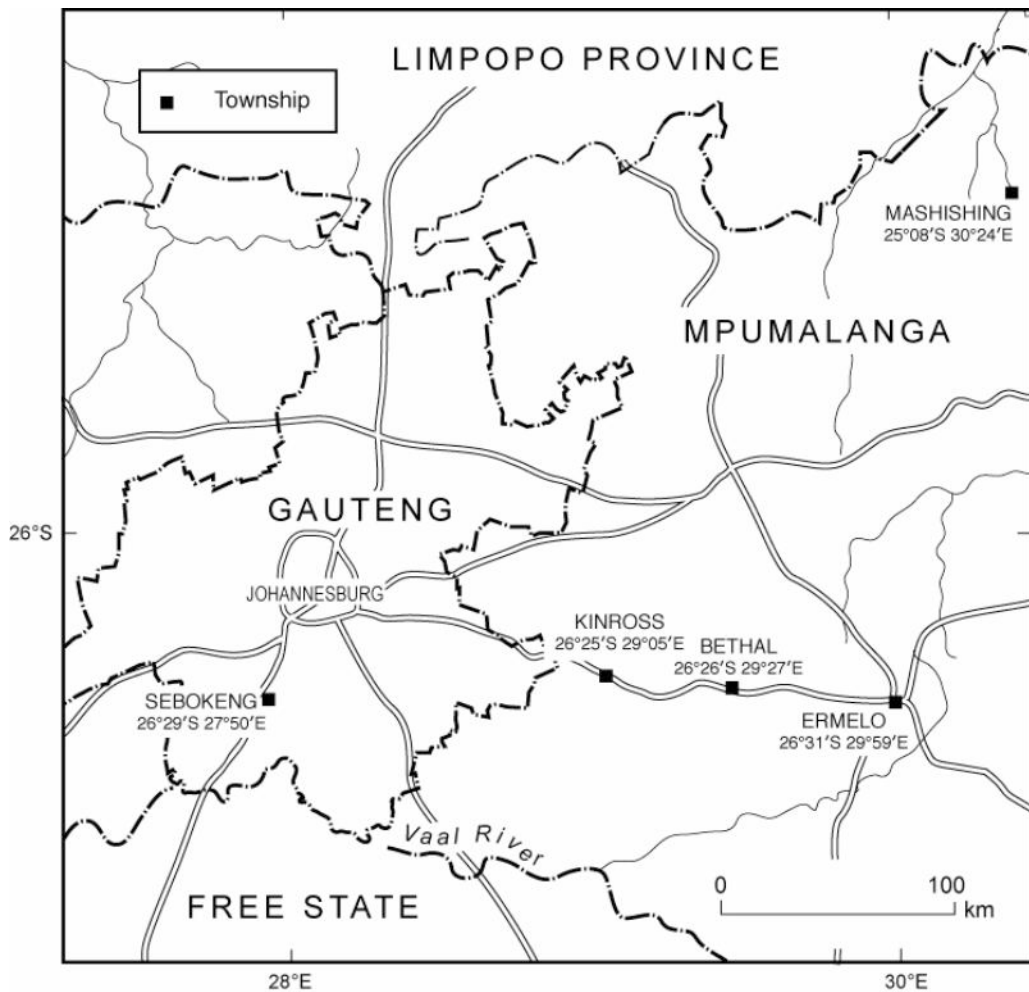


Figure 3.13: Map of the township sites showing their positions relative to each other

Table 3.1: Correlation matrices at AOT_{530nm} measured at township sites in winter and summer 2002

Winter 2002					
Site	Bethal	Ermelo	Kinross	Sebokeng	
Bethal	1	0.02	0.3	0.24	
Ermelo	0.02	1	0.04	0.04	
Kinross	0.3	0.04	1	0.34	
Sebokeng	0.24	0.04	0.34	1	
Summer 2002					
Site	Bethal	Ermelo	Kinross	Sebokeng	Mashishing
Bethal	1	0.14	0.27	0.06	0.2
Ermelo	0.14	1	0.21	0.23	0.02
Kinross	0.27	0.21	1	0.52	0.02
Sebokeng	0.06	0.23	0.52	1	0.01
Mashishing	0.2	0.02	0.02	0.01	1

Industrial/urban sites

. However, a positive correlation co-efficient AOT_{530nm} of between 0.35 and 0.89 in the 2002 summer sampling period was measured between Middelburg, Witbank, Secunda, Springs, and Vereeniging (Table 3.2). These sites (Figure 3.14) were not impacted by local sources and, consequently, reflected a larger scale aerosol loading from transboundary transport.

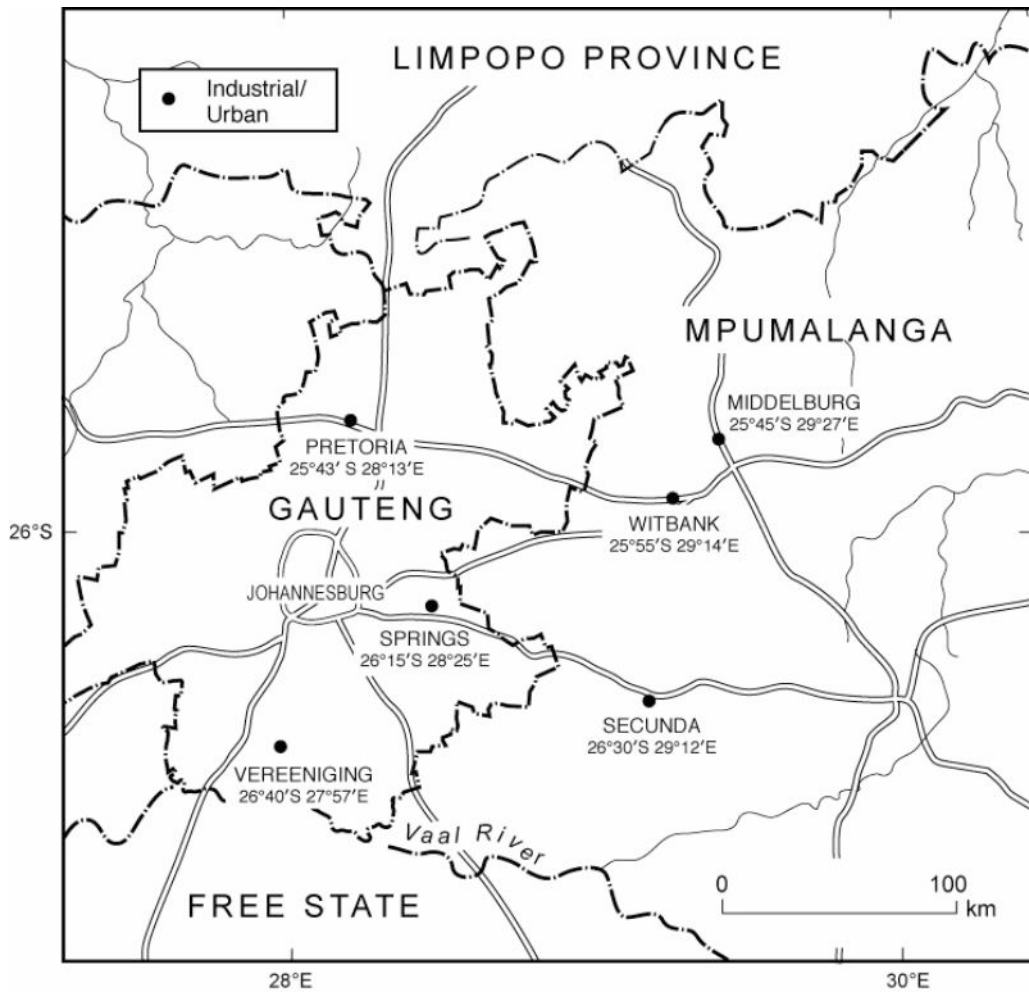


Figure 3.14: Map of the industrial/urban sites showing their positions relative to each other

Table 3.2: Correlation matrices at AOT_{530nm} measured at industrial/urban sites in winter and summer 2002

Winter 2002						
Site	Secunda	Springs	Middelburg	Pretoria	Vereeniging	Witbank
Secunda	1	0.55	0.35	0.01	0.31	0.21
Springs	0.55	1	0.39	0.2	0.34	0.35
Middelburg	0.35	0.39	1	0	0.01	0.46
Pretoria	0.01	0.2	0	1	0.02	0
Vereeniging	0.31	0.34	0.01	0.02	1	0.04
Witbank	0.21	0.35	0.46	0	0.04	1
Summer 2002						
Site	Secunda	Springs	Middelburg	Pretoria	Vereeniging	Witbank
Secunda	1	0.73	0.55	0.11	0.79	0.47
Springs	0.73	1	0.17	0.05	0.7	0.3
Middelburg	0.55	0.17	1	0.25	0.4	0.86
Pretoria	0.11	0.05	0.25	1	0.36	0.56
Vereeniging	0.79	0.7	0.4	0.36	1	0.51
Witbank	0.47	0.3	0.86	0.56	0.51	1

Agricultural sites

In the winter 2002 sampling period, none of the sites correlated, even though they were geographically fairly close to each other (Figure 3.15). This suggested that the aerosol loading was localised at all the sites (Table 3.3). There was a positive weak correlation between Marble Hall and Elias Motsaledi in summer (due to their close proximity) but the AOT_{530nm} at Bela-Bela did not correlate with the other two sites.

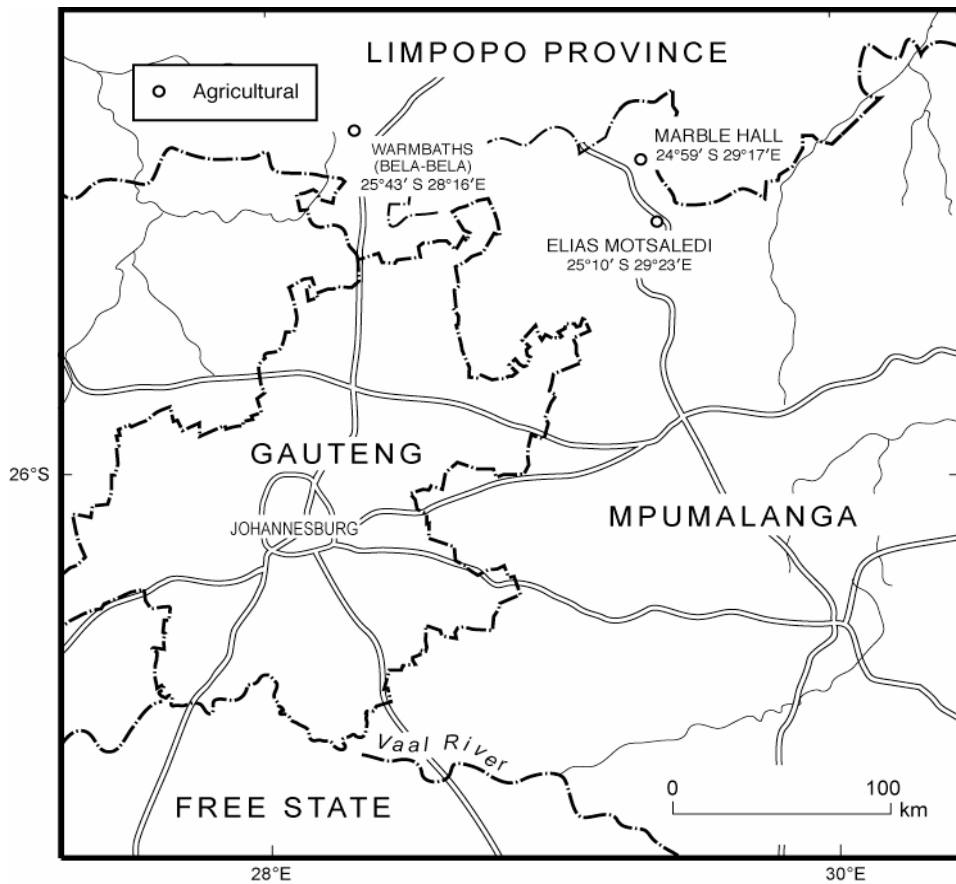


Figure 3.15: Map of the agricultural sites showing their positions relative to each other

Table 3.3: Correlation matrices at AOT_{530nm} measured at agricultural sites in winter and summer 2002

Winter 2002			
Site	Bela-Bela	Elias Motsaledi	Marble Hall
Bela-Bela	1	0.01	0.33
Elias Motsaledi	0.01	1	0.1
Marble Hall	0.33	0.1	1
Summer 2002			
Site	Bela-Bela	Elias Motsaledi	Marble Hall
Bela-Bela	1	0.04	0.01
Elias Motsaledi	0.04	1	0.18
Marble Hall	0.01	0.18	1

Seasonal variation in aerosol size across the Highveld

Sun photometer measurements, taken at different wavelengths of light, provide information not only of the total column aerosol loading, but also the relative amount of the dominant aerosol size within the atmospheric column. Ångström exponent values (Chapter 2) were calculated for all sites during the measurement period. Generally, in the periods recorded, the Highveld was dominated by fine-mode aerosols. During the winter 2002 sampling period, Ångström exponent values of between 1.6 and 2 dominated and typically in the fine fraction, indicating that the aerosols were predominantly from combustion processes. During the summer 2002 sampling period, the Ångström exponent shifted towards lower values, with ~50 % of days dominated by values between 1.2 and 1.4. This shift towards smaller values reinforced the importance of airborne dust in the summer 2002 sampling period (Figure 3.16). The Ångström exponent for the different site categories also confirmed the influence of dust aerosols on the AOT_{530nm} over the Highveld during the summer 2002 sampling period. Ångström exponent values dropped to 1.2 at agricultural sites during the summer 2002 sampling period. A value of an Ångström exponent of <1 would indicate almost exclusively coarse-mode aerosols (aerosols between 2.5 and 10 μm). The Ångström exponent values were highest in the industrial/urban regions, where the predominance of fine-mode secondary aerosols (such as sulphates) could be expected.

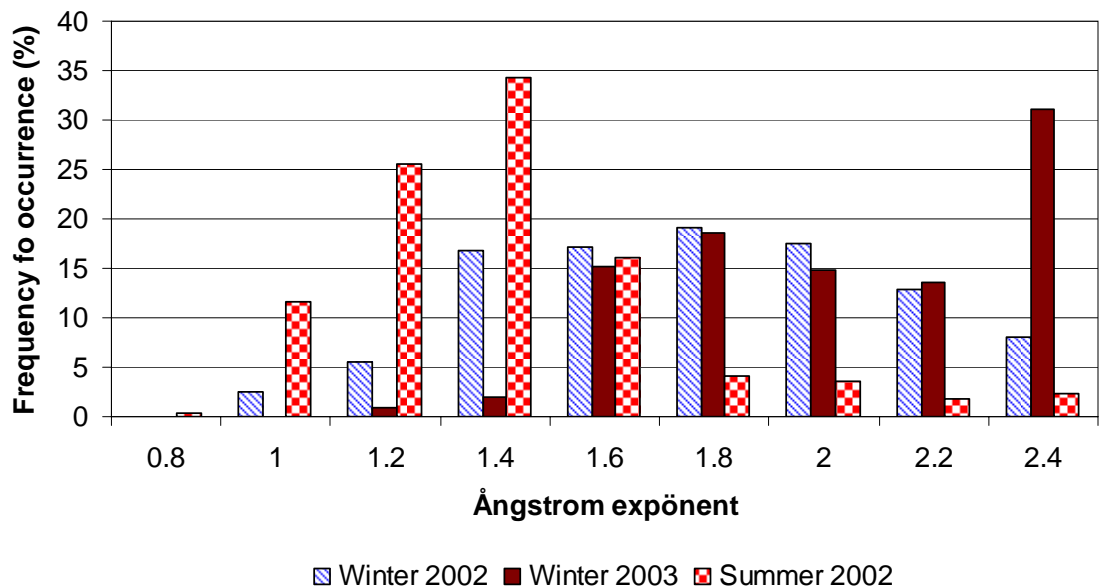


Figure 3.16: Frequency of occurrence of Ångström exponent in winter and summer 2002 and winter 2003 during the entire experiment

Comparison of Ångström exponent in winter and summer between township, industrial/urban and agricultural sites

Township sites

The Ångström exponent over the township sites ranged between 1 and 2.4 in the winter and summer sampling periods (Figures 3.17 and 3.18) respectively. There was a large difference in Ångström exponent between the winter and summer sampling periods. In the summer 2002 sampling period, most of the values were <1.6 with a modal value of 1.2. This means that there was a noticeable shift towards coarse-mode aerosols over the township sites during summer. A reduction in fine AOT_{530nm} particles was visible due to the absence of coal smoke in summer. These particles originated from suspended dust (from unpaved roads) dominating the aerosol loading in these areas, and hence larger aerosols being observed in the measurements.

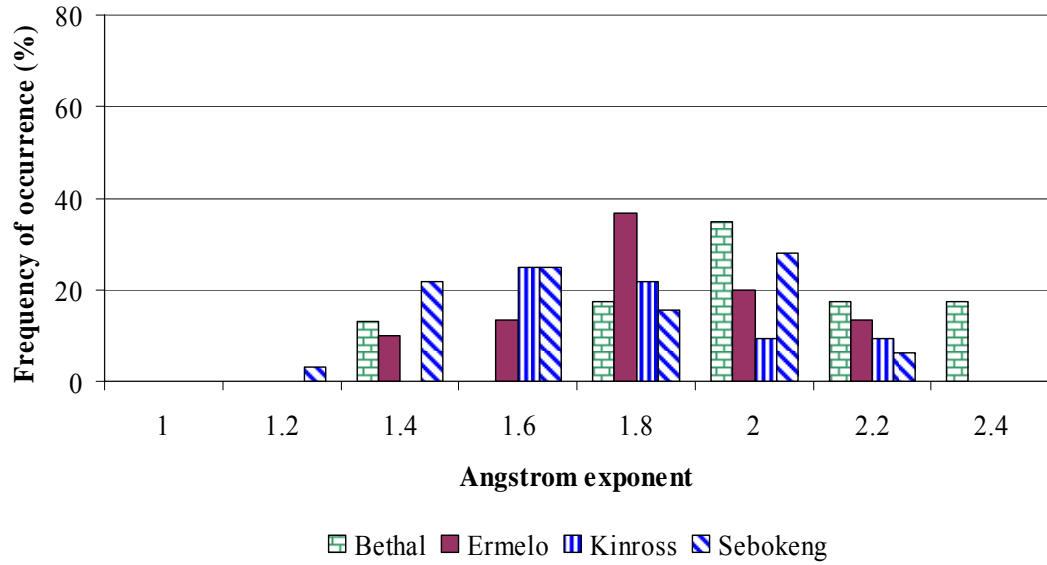


Figure 3.17: Frequency of occurrence of Ångström exponent in winter 2002 for township sites

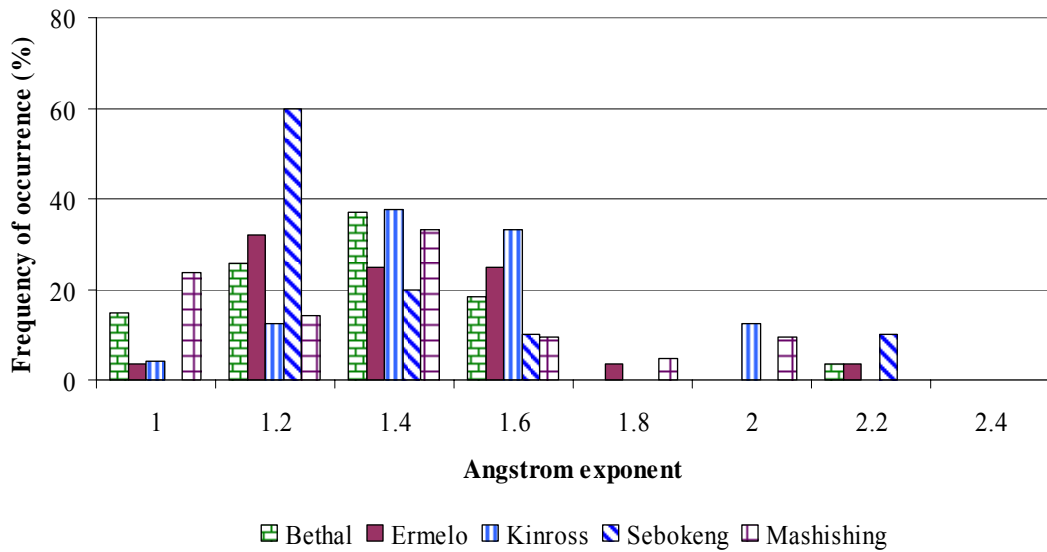


Figure 3.18: Frequency of occurrence of Ångström exponent in summer 2002 for township sites

Industrial/urban sites

At industrial/urban sites, the Ångström exponent was predominantly >1 , ranging between 0.8 and 2.4 (Figure 3.19 and 3.20, respectively). The Ångström exponent was higher (at almost all sites) in the winter 2002 sampling period than in the summer 2002 sampling period. Since industrial output was fairly constant, the increase in fine particles was associated with a more regional air mass in the winter months (Tyson, 1997). The shift in the dominant aerosol sizes between the seasons can best be explained by changes in meteorological and atmospheric conditions.

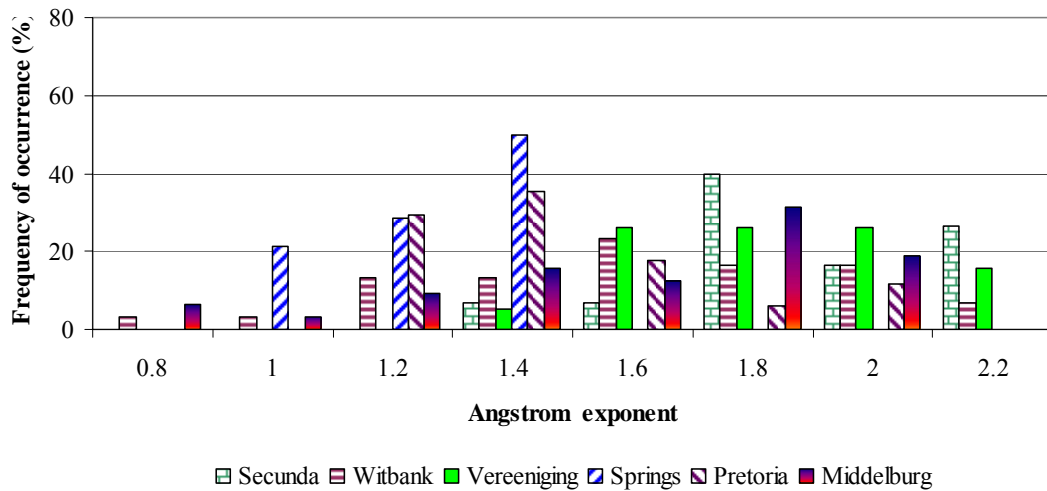


Figure 3.19: Frequency of occurrence histograms of Ångström exponent in winter 2002 for industrial/urban sites

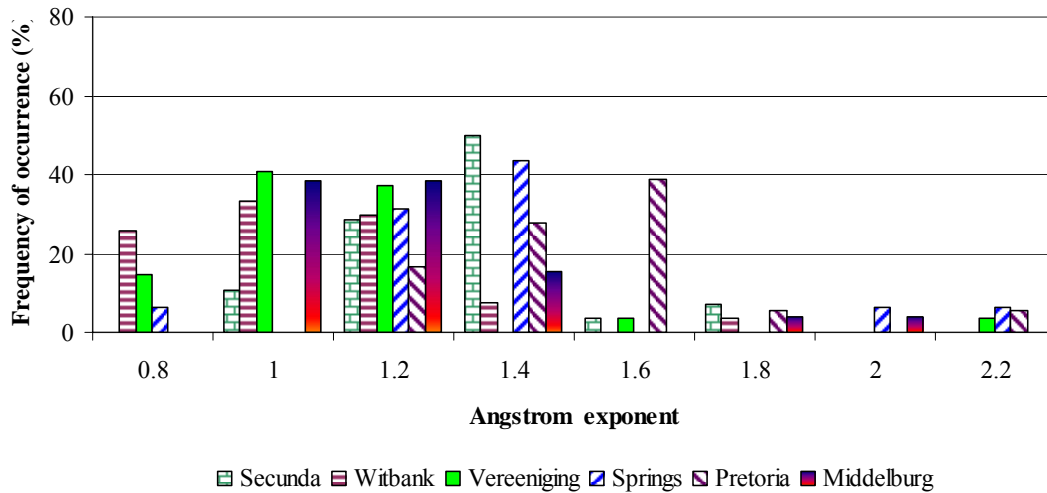


Figure 3.20: Frequency of occurrence histograms of Ångström exponent in summer 2002 for industrial/urban sites

Agricultural sites

In both the winter and summer 2002 sampling periods, the Ångström exponent ranged between 1 and 2.4 (Figures 3.21 and 3.22, respectively). Higher Ångström exponent values were observed at Bela-Bela than at Marble Hall and Elias Motsaledi (especially in winter). The latter sites are more northerly, whilst Bela-Bela is situated further west.

The results at Bela-Bela were characteristic of small particles originating from biomass burning that takes place mainly in late winter (Eck *et al.*, 2003). In the summer 2002 sampling period, at Bela-Bela there was a shift in Ångström exponent values towards the coarse-mode aerosols.

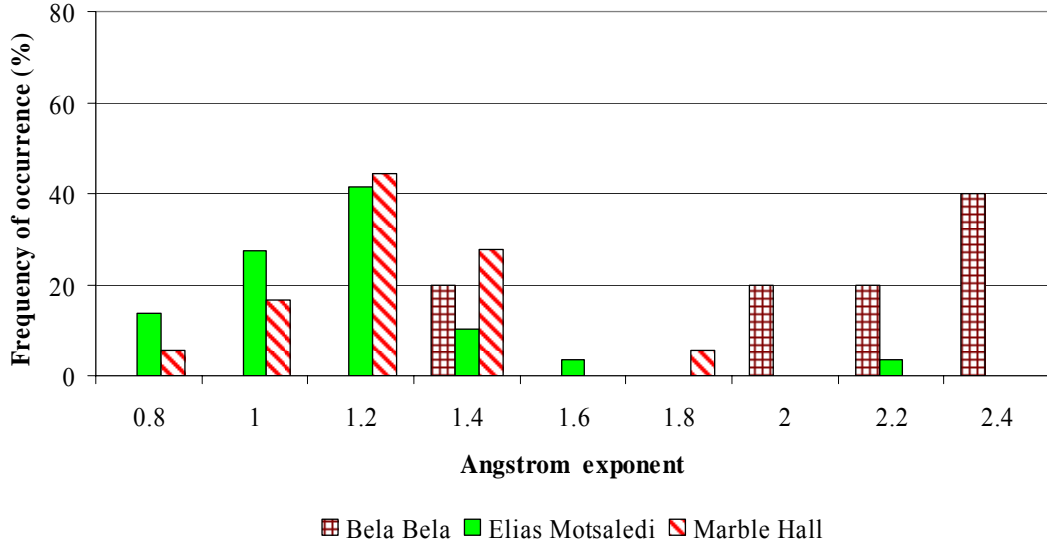


Figure 3.21: Frequency of occurrence histograms of Ångström exponent in winter 2002 for agricultural sites

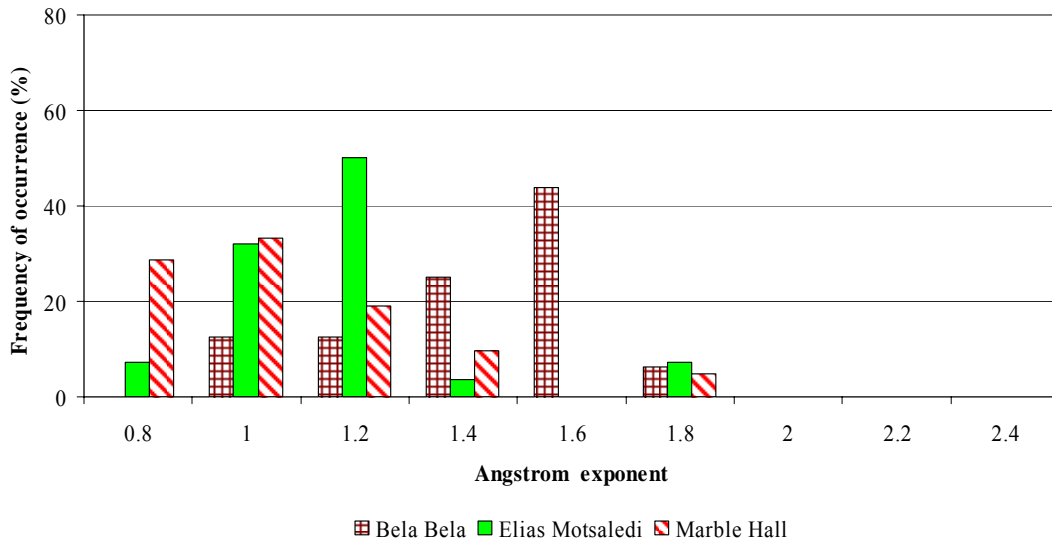


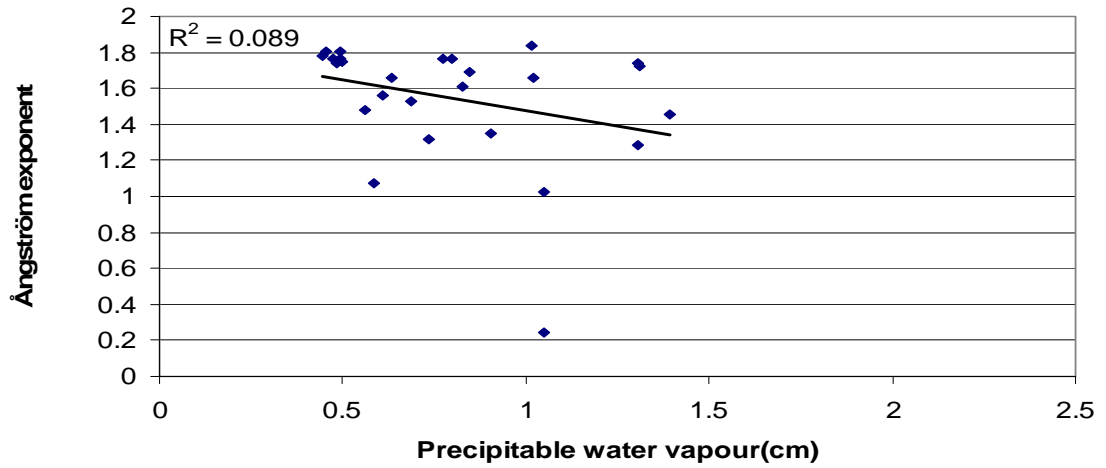
Figure 3.22: Frequency of occurrence histograms of Ångström exponent in summer 2002 at agricultural sites

Ångström exponent and precipitable water vapour content in winter and summer

In order to evaluate the influence of water vapour on aerosols, the relationship between Ångström exponent and precipitable water vapour was examined (Figure 3.23). During the 2002 winter and summer sampling periods, the results indicated no direct correlation between winter and summer ($r^2 = 0.09$ and $r^2 = 0.15$, respectively), thus suggesting that part of the reason may be that aerosol and water vapour are transported at different altitudes over the Highveld region and/or that there are trajectories from several source regions with differing seasonal combinations of aerosols and precipitable water vapour.

De Tomasi and Perrone (2003) carried out an experiment investigating the temporal and spatial relationship among the aerosol backscattering ratio and the water vapor mixing ratio, over southeastern Italy. The analysis of the lidar data revealed a strong correlation between the spatial and temporal evolution of AOT and water vapour both in summer and in autumn regimes. It was found that AOT increased with water vapour and that both reduced as a result of the transition between summer and autumn regime. It was also observed that the correlation among AOT and water vapour was dependent on the air masses origin. Indeed, the sensitivity of the scattering ratio to water vapor changes was larger for the air masses advected from North and East European Countries (De Tomasi and Perrone, 2003)

a)



b)

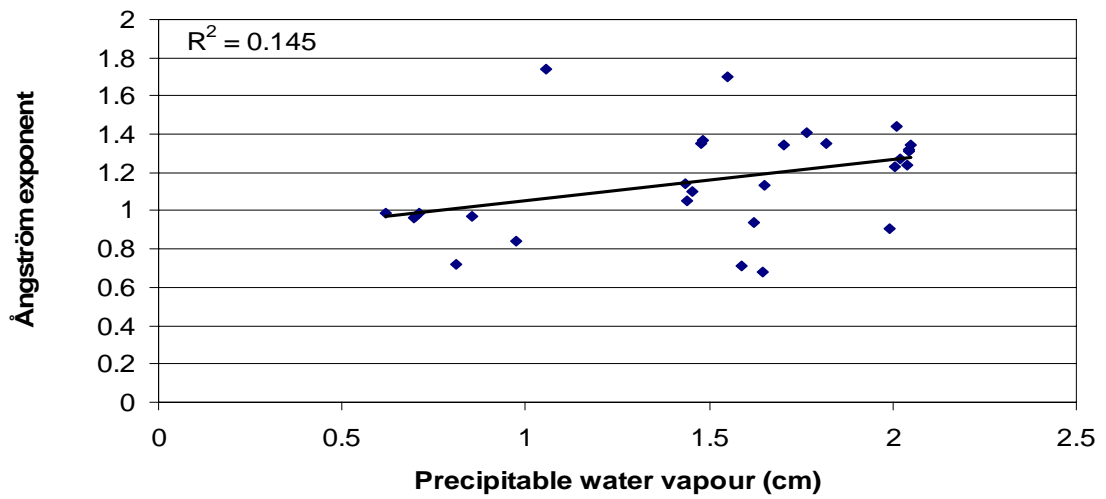


Figure 3.23: Ångström exponent versus water vapour variability in a) winter 2002 and b) summer 2002

AOT_{530nm} over the Highveld was higher in the summer sampling period than in winter sampling periods. It was generally low for an industrial/urban environment which produces more fine- than coarse-mode particles. Aerosol characteristics were fairly homogeneous across the Highveld, especially in the winter sampling period, indicating well-mixed air masses. AOT_{530nm} increased across the Highveld from a southwest to a northeast direction.

CHAPTER 4:

SYNOPTIC CIRCULATION AND ATMOSPHERIC TRANSPORT

The synoptic systems affecting the Highveld region of South Africa will be discussed. The atmospheric transport patterns influencing the aerosol loading over the Highveld will be considered in this chapter. Kinematic trajectory analysis will be used to understand the modes of transport of material into and within the Highveld region. Case studies of some atmospheric events will be discussed for the township sites.

Frequency of occurrence of atmospheric transport systems during the Highveld Haze Project (2002 to 2003)

Backward trajectory analysis at 850, 700 and 500 hPa showed three transport pathways prevailed over the Highveld during the winter 2002 sampling period. In the summer 2002 sampling period, four transport pathways prevailed over the Highveld: easterly waves (50 %); continental anticyclones (30 %); ridging highs (10 %), and occasionally westerly waves (9 %) (Figure 4.1). The high incidence of easterly waves in summer is supported by other researchers (Tyson *et al.*, 2000; Freiman and Piketh, 2003). In the winter 2002 sampling period, by contrast, easterly waves did not occur, but continental anticyclones dominated (56 %); followed by ridging highs (27 %), and westerly waves (15 %) (Figure 4.1).

Variations in the spatial and temporal concentration of aerosols have been found to be associated with different air mass transport pathways over South Africa (Garstang *et al.*, 1996; Tyson *et al.*, 1996; Tyson, 1999). Four main circulation types dominate atmospheric circulation over South Africa, with varying frequencies throughout the year, resulting in different air mass transport pathways (Tyson *et al.*, 1996).

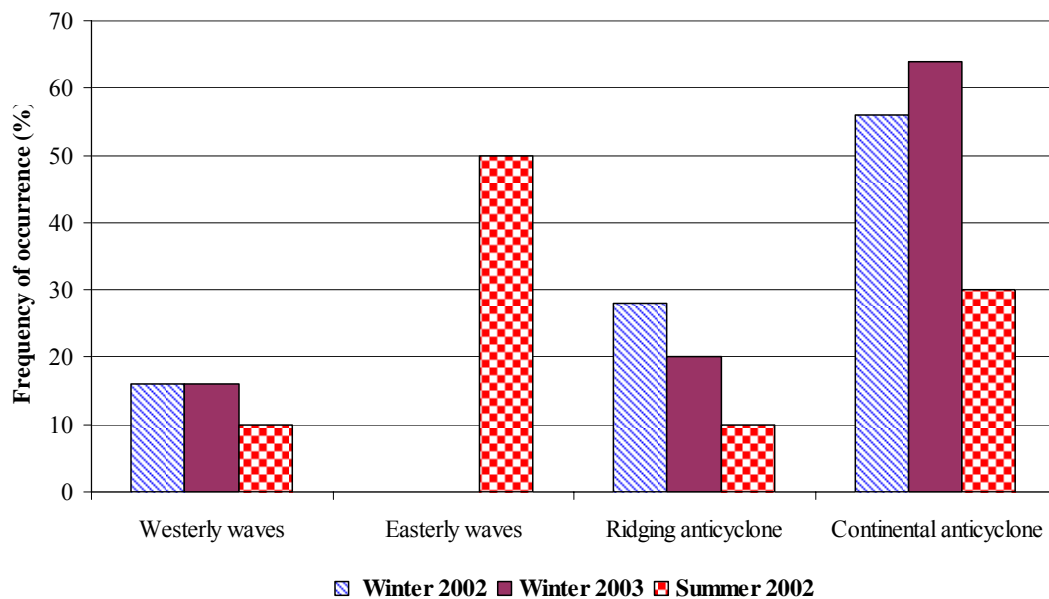


Figure 4.1: Synoptic surface frequency of occurrence over the Highveld region in winter 2002, winter 2003 and summer 2002

Atmospheric transport over the Highveld during the winter and summer 2002 sampling periods selected using case studies from the township sites

The selected case studies have been used to show how the combination of cold fronts versus anti-cyclonic weather phenomena brought about low and high AOT loading over the township sites throughout the sampling periods.

Winter 2002

Fine weather conditions persist for ~80 % of the year over South Africa in winter (Schulze, 1965; Harrison, 1984), encouraging the development of absolutely stable layers in the atmosphere. The predominantly stable troposphere (Figure 4.2) promotes the trapping of material between these stable layers.

Stable tropospheric conditions only abate with either deep convection (and the concurrence of unstable barotropic easterly disturbances), or with the passage of intense baroclinic westerly disturbances (Freiman and Tyson, 2000). During the winter 2002 sampling period, episodes of high AOT_{530nm} were recorded on 10 June, 17 June, and 21 June. However, between 12 June and 14 June, a cold front passed over the Highveld (Figure 4.3), precipitating a drop in AOT_{530nm} . The average AOT_{530nm} (Figure 4.4) was 0.12 ± 0.07 , whilst the Ångström exponent for this period was 1.79 ± 0.29 .

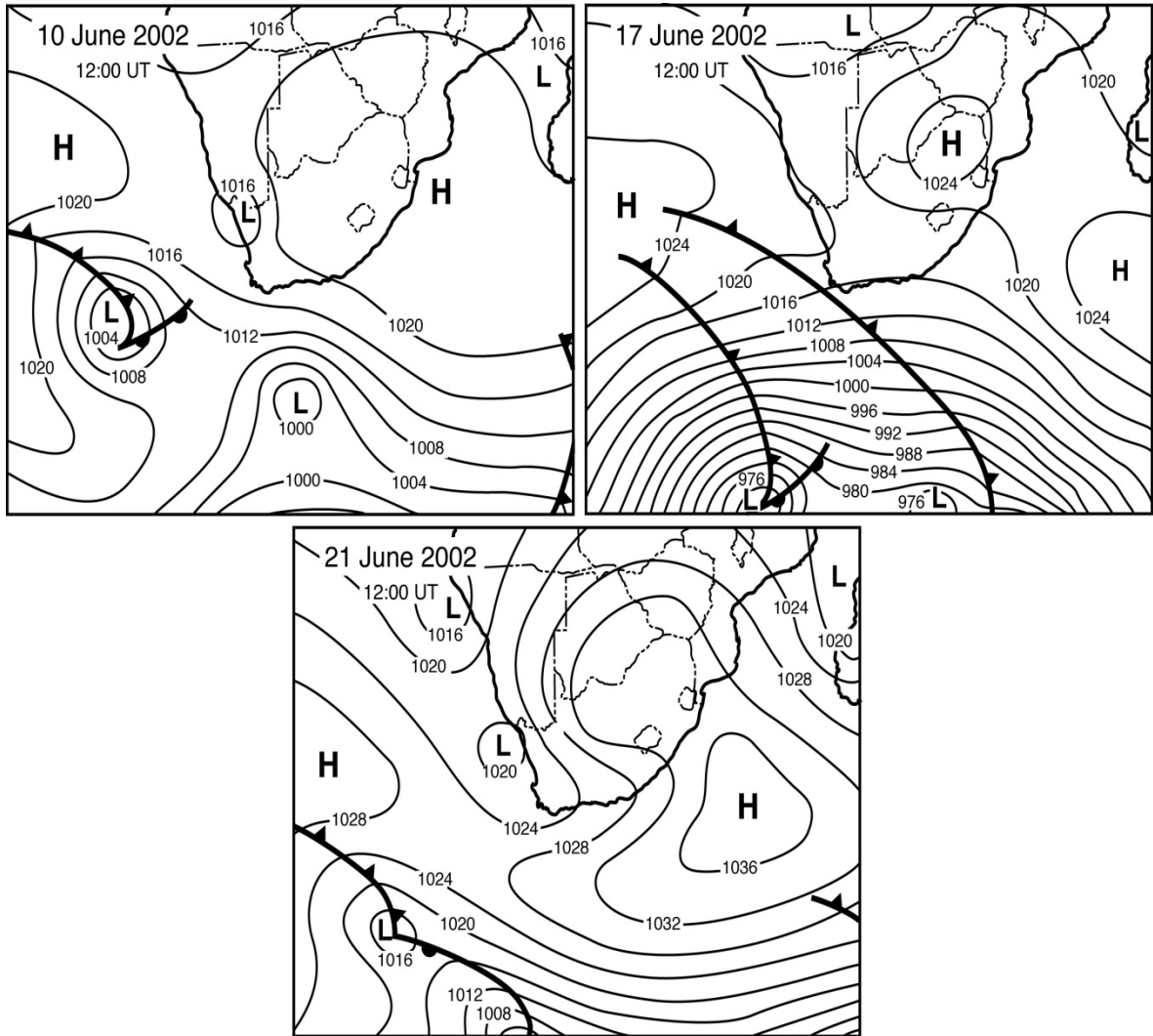


Figure 4.2: Surface weather charts on a) 10 June, b) 17 June and c) 21 June 2002 showing conditions conducive for AOT build-up over township sites

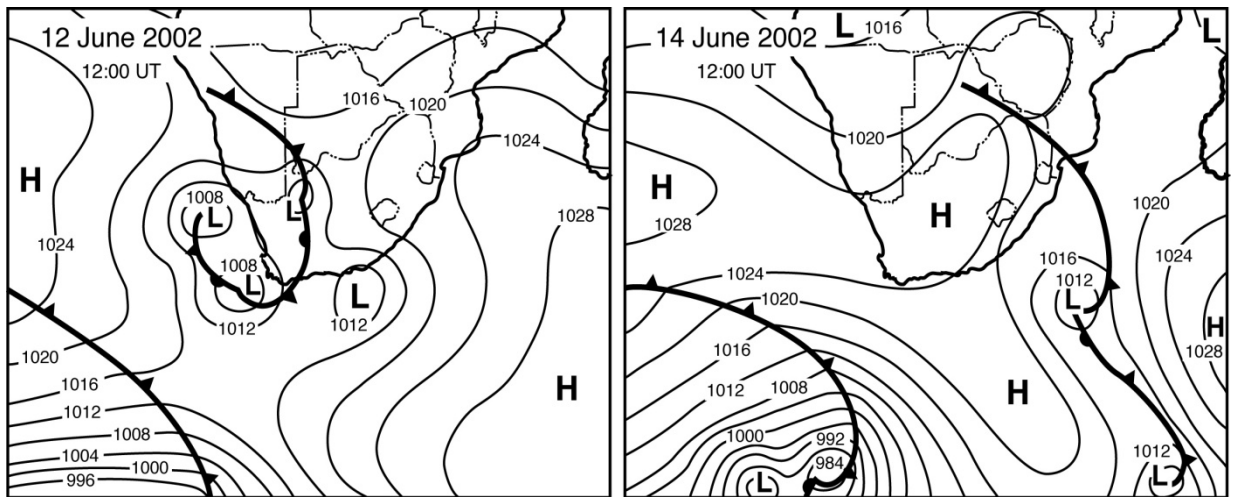


Figure 4.3: Surface weather charts on a) 12 June and b) 14 June 2002 showing cold front conditions over township sites

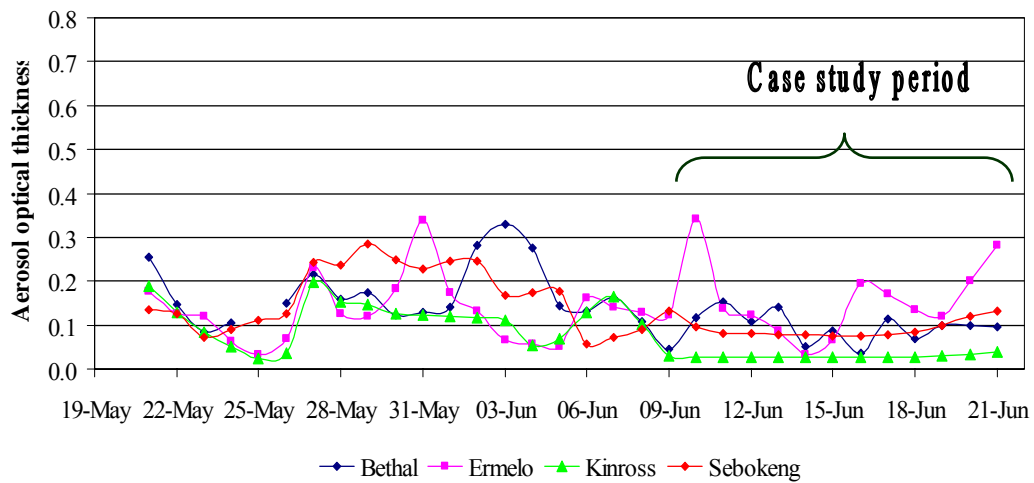
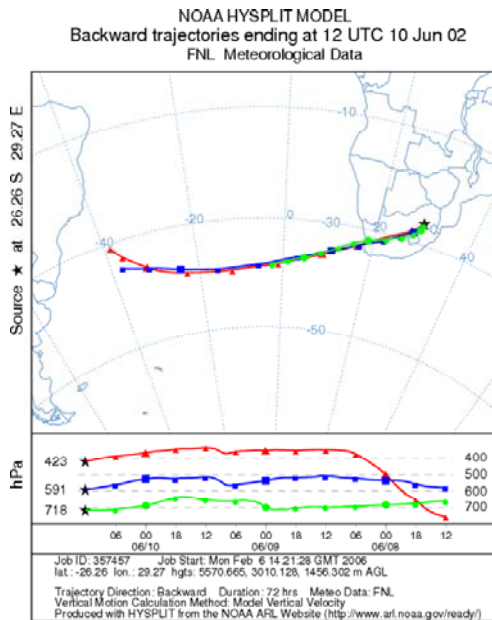


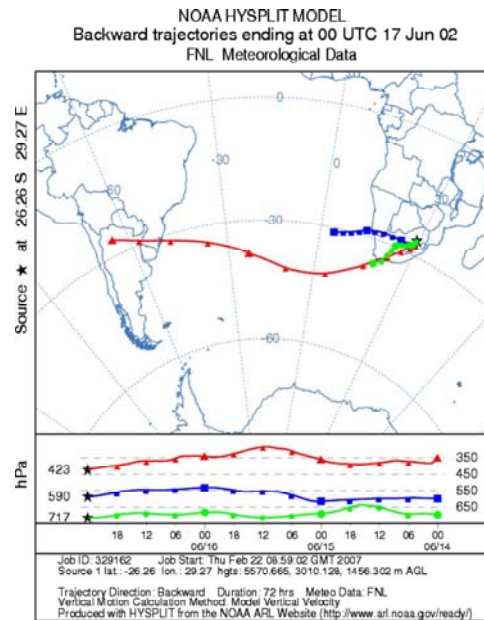
Figure 4.4: Aerosol optical thickness measurements for winter 2002 sampling period over township sites

Trajectory analysis was run at 850, 700 and 500 hPa levels (Figure 4.5). The high Ångström exponent (1.79) might have been due to emissions from township and agricultural sites in the area. The possible source of these emissions was the burning of waste (which had been dumped at the township outskirts) and dry vegetation along road verges within the township sites (especially at Bethal and Ermelo).

a)



b)



c)

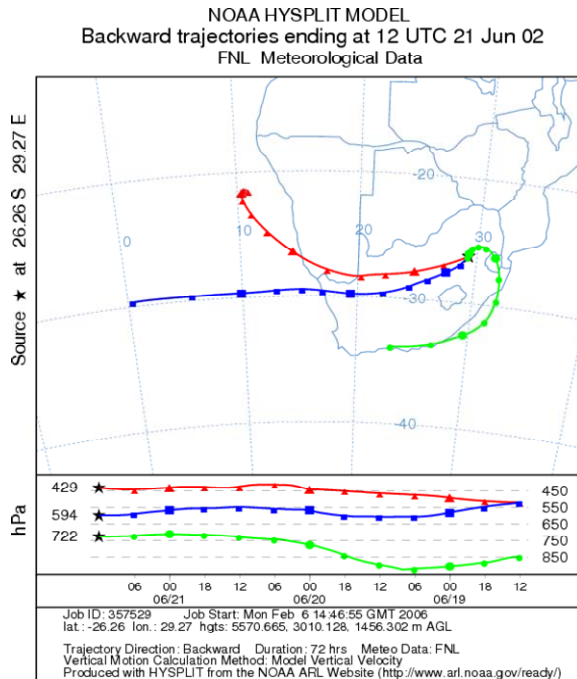


Figure 4.5: Four-day backward trajectory in winter 2002 showing transport into the Highveld on a) 10 June, b) 17 June and c) 21 June at 800, 700 and 500 hPa under conditions favourable for AOT build-up

Between 2 June and 8 June, there was a high degree of AOT_{500nm} levels over the township sites (Figure 4.6). This was related to a combination of a Continental high and cold front present over the country at this time. (Figure 4.7). The high Ångström exponent (2) may have been due to biomass products being advected into and over the Highveld from the north-northwest (Freiman and Tyson, 2000). The average AOT_{500nm} recorded was 0.22 ± 0.09 while the Ångström exponent average was 2.03 ± 0.25 .

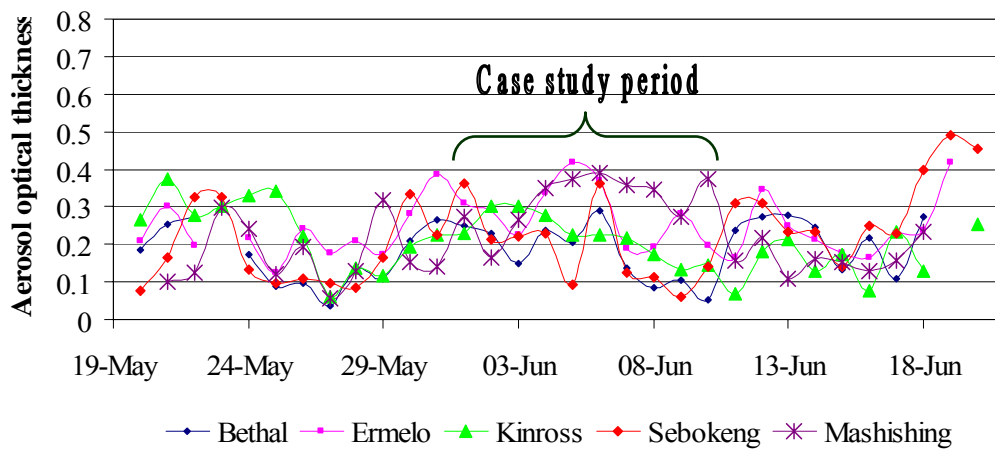


Figure 4.6: Aerosol optical thickness measurements for winter 2003 over township sites

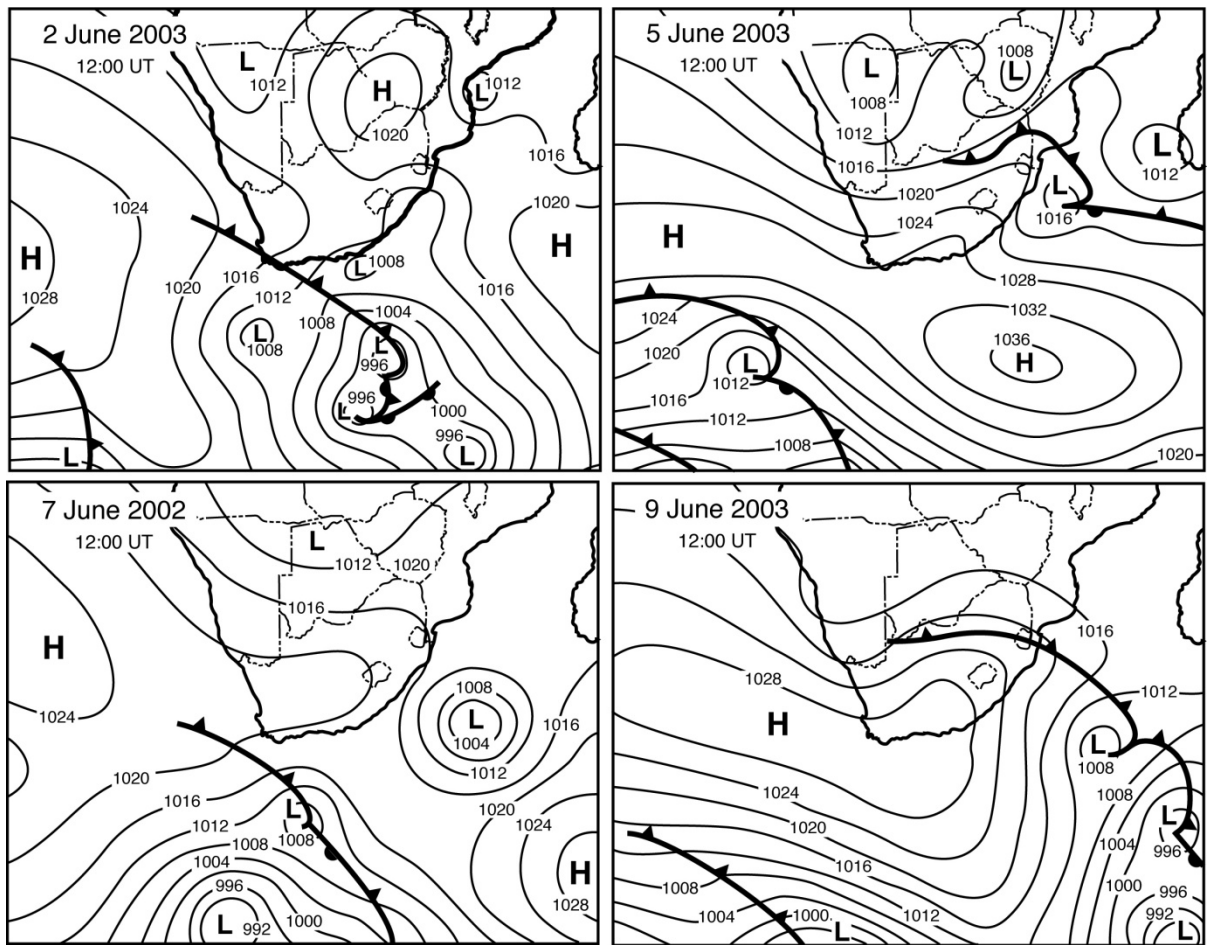


Figure 4.7: Surface weather charts on a) 2 June, b) 5 June, c) 7 June and d) 9 June 2003 showing a cold front over the Highveld region

The analysis from the trajectories (at 850, 700 and 500 hPa levels) shows air being advected from the west, which is ideally clean marine air (Figure 4.8). However, the high Ångström exponent (2) was possibly due to fresh biomass burning material in the region.

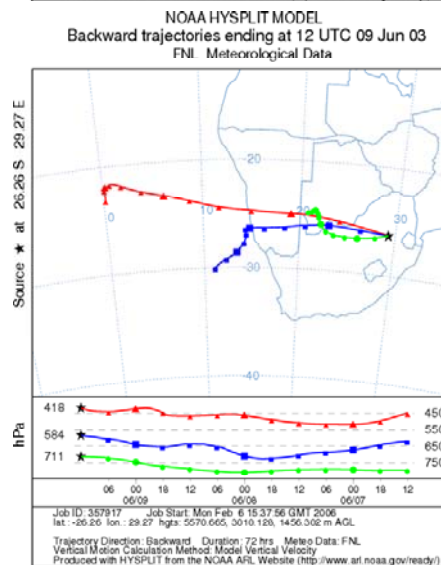
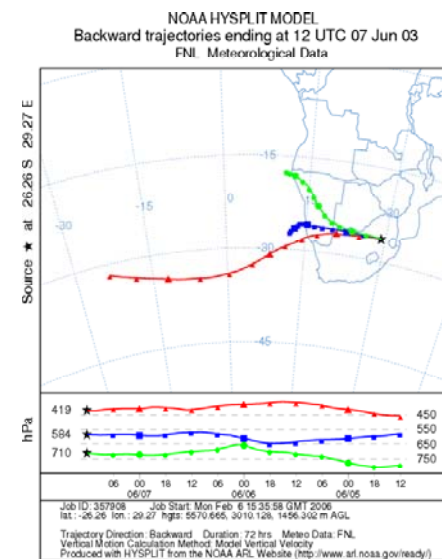
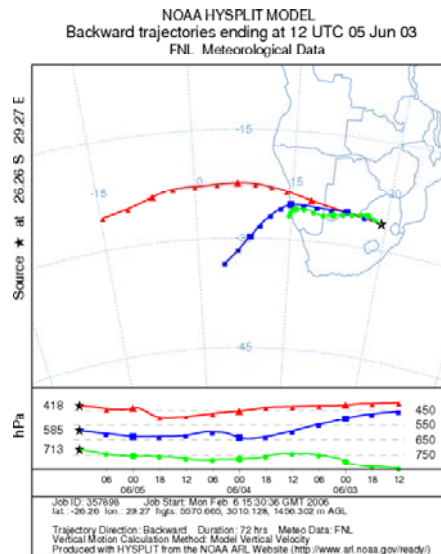
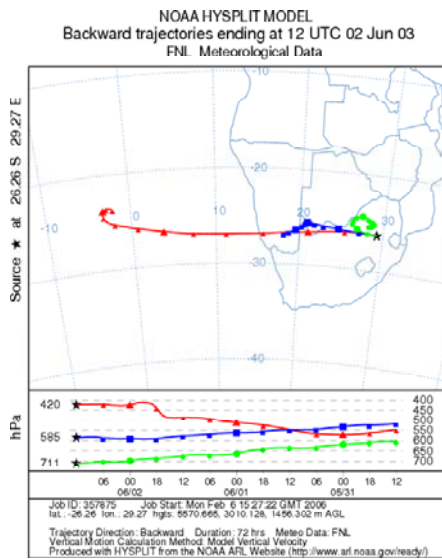


Figure 4.8: Four-day backward trajectory in winter 2003 showing transport into township sites for the period 2 to 9 June at 800, 700 and 500 hPa under low AOT conditions

Summer 2002

In the summer of 2002 a number of days were chosen that showed a distinct pattern of low and high loadings. During the high AOT_{530nm} on 24 to 28 October, the average AOT_{530nm} and Ångström exponent was 0.34 ± 0.03 and 1.42 ± 0.32 , respectively (Figure 4.9). A shallow trough prevailed over the interior of the country during this time (Figure 4.10). Low-level convergence occurred to the east of the surface trough, while at 500 hPa or above air diverged (Tyson and Preston-Whyte, 2000). Low AOT_{530nm} days (7 to 13 November) were associated with AOT_{530nm} values of about 0.19 ± 0.04 and an Ångström exponent of 1.33 ± 0.19 . A shallow low-pressure trough was present at this time (Figure 4.12). The low AOT_{530nm} was due to washout from the low-pressure trough that passed over the Highveld. However a different trend is shown in the data for Kinross. This could be due to a local burning episode (biomass or domestic coal use).

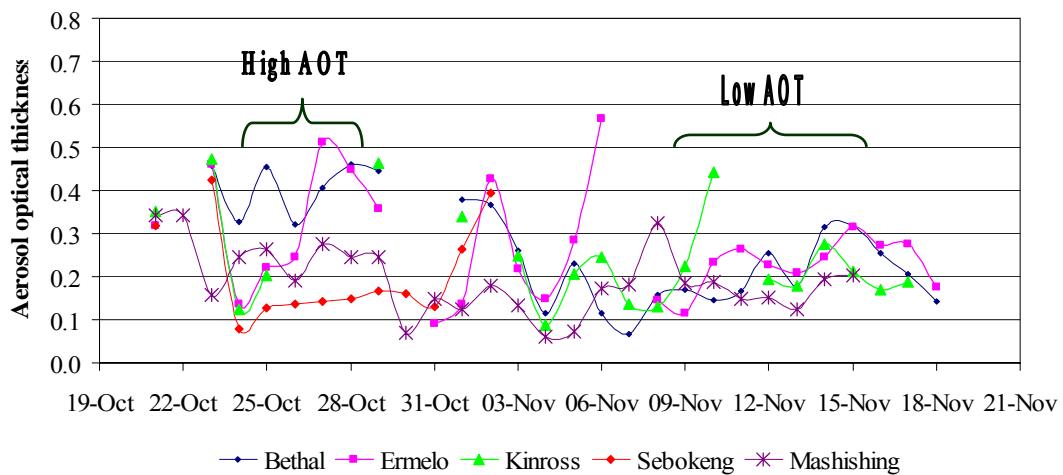


Figure 4.9: Aerosol optical thickness measurements for the summer 2002 sampling period

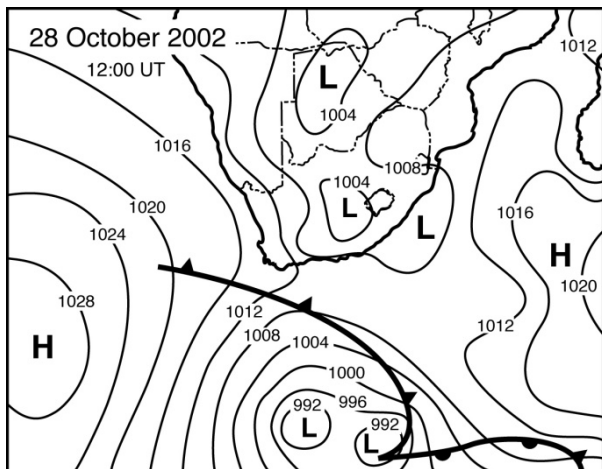


Figure 4.10: Surface weather charts on 28 October 2002 showing a shallow low pressure system over the Highveld region

Trajectory analysis was run at three different levels: 850, 700 and 500 hPa (Figure 4.11). Air was advected into the sampling sites from neighbouring states. This is shown in the Ångström exponent values measured over the Highveld. These values may be due to biomass burning aerosols of small particle size either from local sources or from long-range transport from Mozambique and Botswana. This could also be associated with pronounced ridging behind a cold front, where some recirculation may have occurred (Freiman and Piketh, 2003).

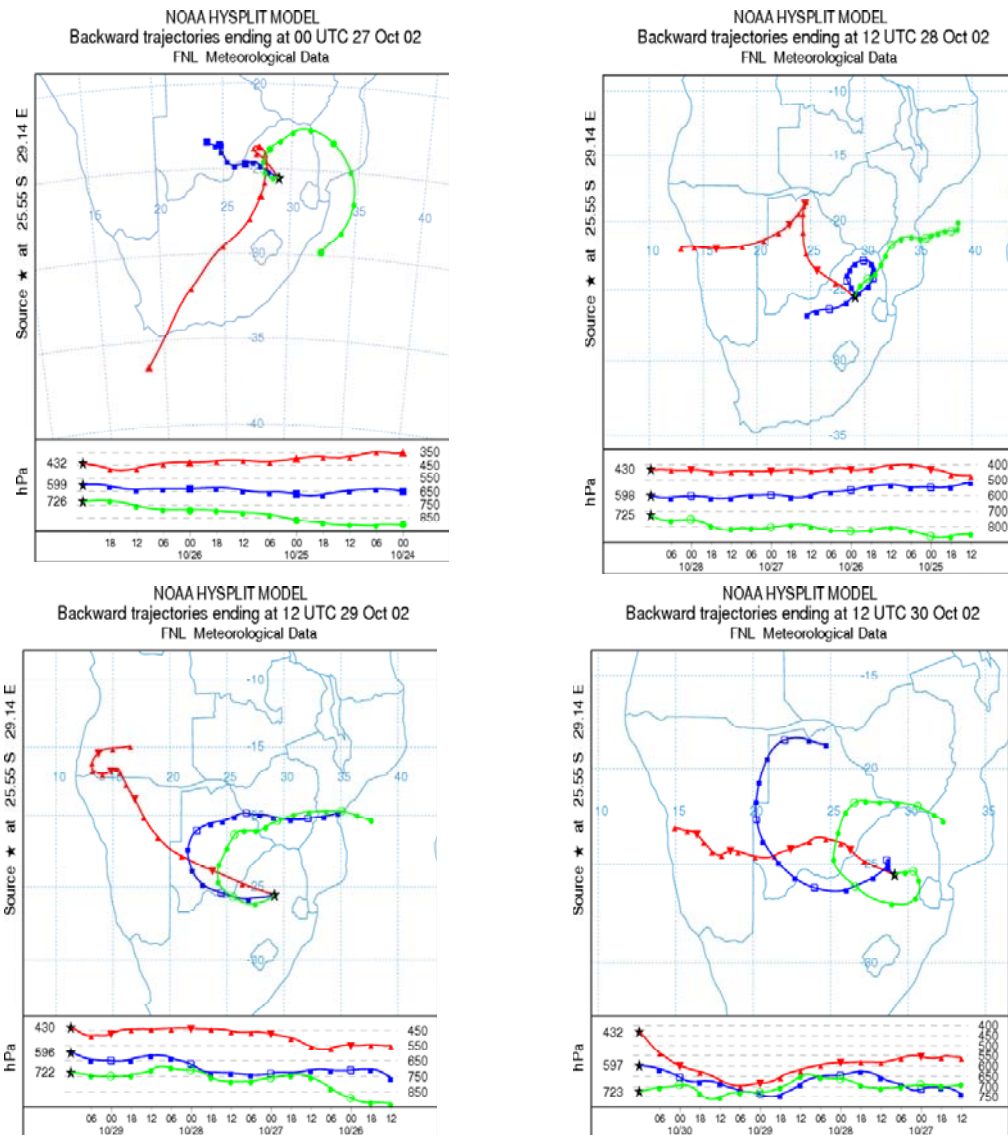


Figure 4.11: Four-day backward trajectory in summer 2002 showing transport into the Highveld for the period 27 to 30 October at 800, 700 and 500 hPa

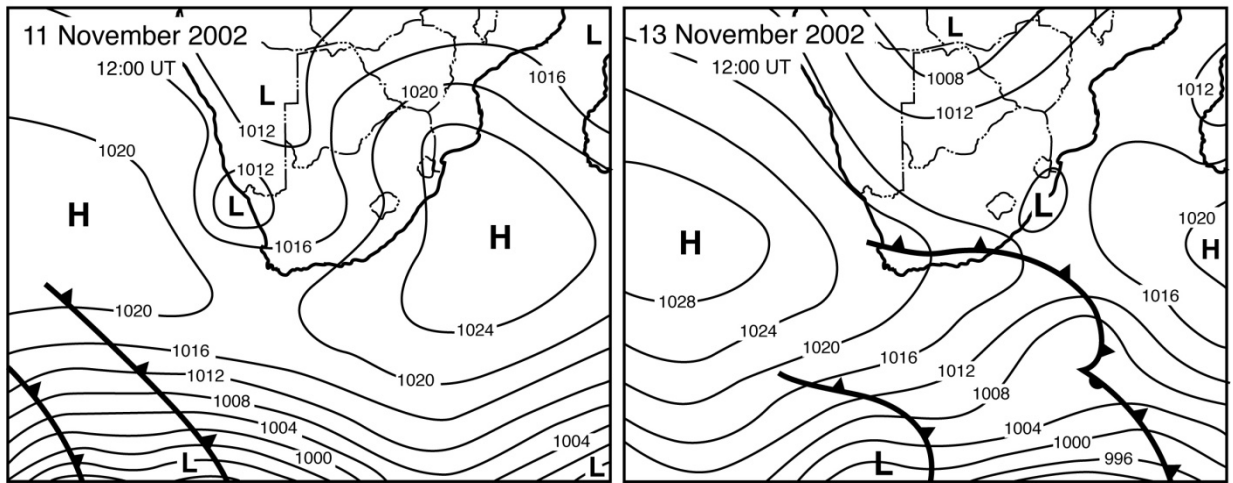


Figure 4.12: Surface weather charts on a) 11 November and b) 13 November showing a shallow low pressure system over the Highveld region

Trajectory analysis was also run at 850, 700 and 500 hPa levels (Figure 4.13). Air from the south Atlantic is normally free from emissions (Freiman and Piketh, 2003). This explains the low AOT_{530nm} measured.

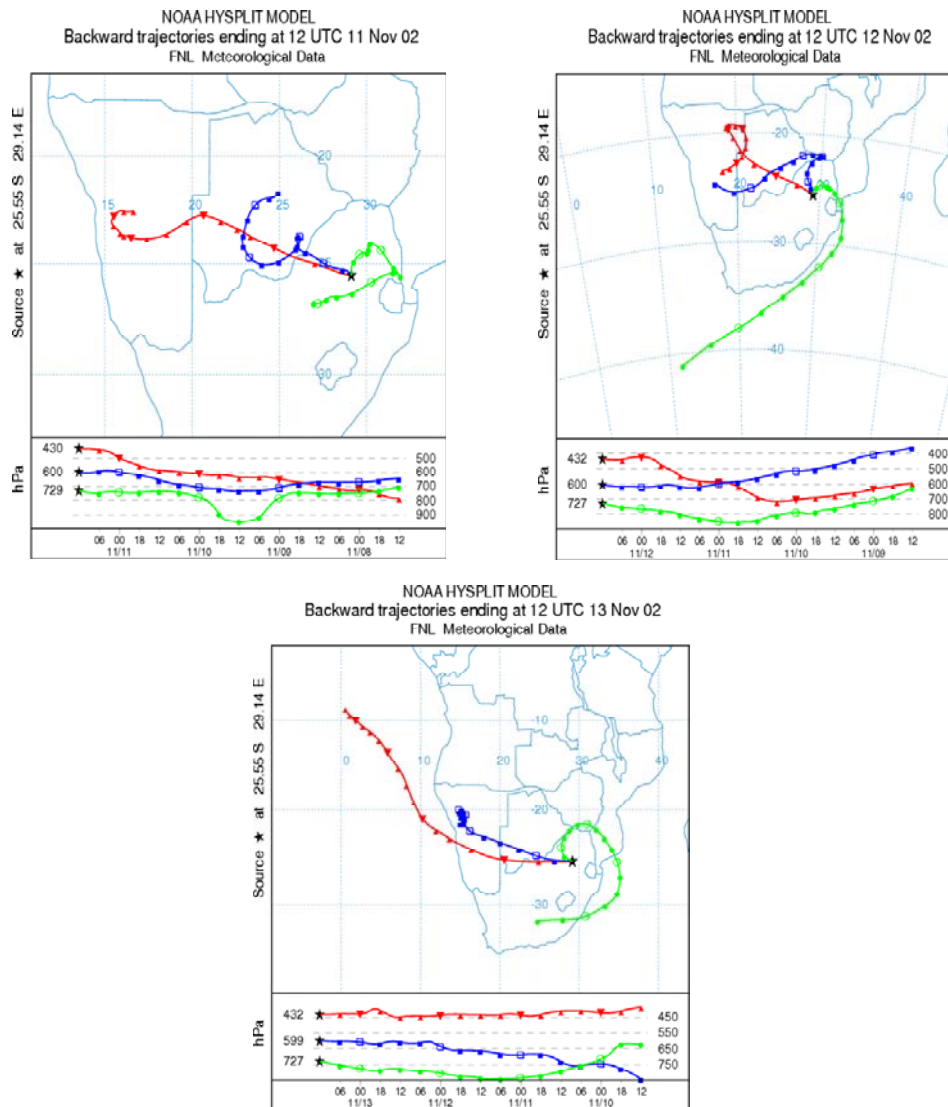


Figure 4.13: Four-day backward trajectory in summer 2002 showing transport into the Highveld for the period 11 to 13 November at 800, 700 and 500 hPa under low AOT conditions

The dominant transport pathway in winter was the continental flow while easterly waves were most prevalent in summer. Backward-trajectory analysis at 850, 700 and 500 hPa over the Highveld region during winter and summer 2002 indicated north-westerly to westerly wave transport pathways into the Highveld as computed from the data. Three case studies for township sites were discussed, based on the effects of the combination of a cold front versus an anti-cyclonic weather phenomenon.

CHAPTER 5:

SUMMARY AND CONCLUSION

A number of important findings has been drawn from this study relating to aerosol loading over the South African Highveld. These are discussed below.

The Highveld region is South Africa's major industrial area. This region plays a major role in the production and transport of aerosols. The township areas, industrial/urban areas, and agricultural areas in this region are important source emitters of sulphur, carbon, nitrogen and their corresponding oxides. The spatial distribution of aerosol loading over the Highveld has been analysed. This was done during winter and summer, over 32 days, in three distinct collection periods: May to June 2002; October to November 2002, and May to June 2003. The principal findings of the study are:

1. The highest AOT_{530nm} was recorded in the summer 2002 sampling period at the township sites (≥ 0.6), while the AOT_{530nm} across all sites never exceeded 0.5 in the winter sampling periods. The impact of aerosol loading at these sites during the summer sampling period was due to high atmospheric dust.
2. At industrial/urban sites higher AOT_{530nm} levels were recorded in the winter sampling periods for all sites (when compared to the summer sampling period levels). The high AOT_{530nm} was possibly due to a high concentration of industries near the sampling sites. Coupled with the meteorological conditions, these results are characteristic of winter.
3. At the agricultural sites, during the summer sampling period, there was variability of aerosol loading at each site.

4. During the summer sampling period, easterly waves dominated, followed by continental anticyclones, then ridging highs and cut-off lows. In the winter sampling period, continental anticyclones dominated, followed by ridging highs and then westerly waves.
5. The wind speeds during the summer sampling period were slightly higher than during the winter sampling periods. During the summer sampling period, the aerosol loading was impacted by wind-blown dust and possibly high water vapour levels. A shallow low pressure system dominated over the Highveld in the summer sampling period.
6. A cold front dominated the winter 2003 sampling period, at which time the Ångström exponent was high. This may have been due to biomass products being advected into the Highveld region from the north.
7. In the winter 2002 sampling period, fine weather occurred, hence the high AOT_{530nm} and Ångström exponent values recorded at this time.
8. No correlation was noted between the AOT_{530nm} measured at most sites (in their different classifications) throughout the three sampling periods. This may have been due to the AOT_{530nm} being a function of local sources (township- and agricultural- sites). It may also have reflected a larger scale aerosol loading impact (industrial/urban sites).
9. The Ångström exponent in the winter sampling period was dominated by values of between 1.6 and 2, indicating a predominance of combustion aerosols. In the summer sampling period, the Ångström exponent values dropped (~50 % of values were between 1.2 and 1.4). This suggested that dust was a more important source of AOT loading during the summer sampling period.
10. The Ångström exponent values were highest at industrial/urban sites where the predominance of fine-mode secondary aerosols (such as sulphates) would be expected. At township- and agricultural- sites, the values dropped in the summer sampling period, indicating

predominantly coarse-mode aerosols from unpaved roads and agricultural activities.

11. There was no clear relationship between Ångström exponent and precipitable water vapour over the Highveld in either the winter or the summer sampling periods.

Indications are that aerosol loading over southern Africa should not be considered as restricted to the Highveld region as a source, but account should be taken of other contributing factors around the Highveld region.

REFERENCES

- Ackerman, A.S., Toon, O.B., Steven, D.E., Heymsfield, A.J., Ramanathan, V. and Wleton, E.J., 2000: Reduction of tropical cloudiness by soot, *Science*, 288, 1042-1047.
- Andreae, M.O., 1996: "Biomass burning: its history, use and distribution and its impact on environmental quality and global climate". In: *Global Biomass Burning: Atmospheric, Climate and Biospheric Implications*, Levine, J.S. (Ed.), MIT Press, Cambridge, Massachusetts, 213-232.
- Ångström, A., 1961: Techniques of determining the turbidity of the atmosphere, *Tellus*, 13, 214-223.
- Annegarn, H.J., 1997: *A bird's eye view of air pollution issues in South Africa*. National Association for Clean Air, 28th Annual Conference, Iscor Club, Vanderbijlpark, 20 November.
- Annegarn, H.J., Braga-Marcazzan, G.M., Cereda, E., Marchionni, M. and Zucchiatti, A., 1992: Source profiles by unique ratios (SPUR) analysis: Determination of source profiles from receptor-site streaker samples, *Atmospheric Environment*, 26A, 333-343.
- Bohen, C.F. and Huffman, D.R., 1983: *Absorption and scattering of light by small particles*, John Wiley and Sons, New York.
- Brooks, D.R. and Mims III, F.M., 2001: Development of an inexpensive handheld LED-based sun photometer for the Globe Program, *Journal of Geophysical Research*, 106, 4733-4740.
- Charlson, R.J. and Heintzenberg, J., 1995: Foreword. In: *Aerosol Forcing of Climate*, R.J. Charlson and J. Heintzenberg (Eds.), John Wiley and Sons, Chichester, 1-10.

- Charlson, R.J. and Heintzenberg, J. (Eds.), 1995: *Aerosol Forcing of Climate*, John Wiley and Sons, New York.
- Charlson, R.J., 1997: Direct climate forcing by anthropogenic sulphate aerosols: The Arrhenius paradigm a century later, *Ambio*, 26(1), 25-31.
- Charlson, R.J., Langer, J. and Rodhe, H., 1990: Sulphate aerosol and climate, *Nature*, 326, 655-661.
- Chimidza, S. and Moloi, K., 2000: Identification of sources of aerosol particles in three locations in eastern Botswana, *Journal of Geophysical Research*, 105, 17811-17818.
- Chin, M., Ginoux, P., Kinne, S., Torres, O., Holben, B.N., Duncan, B.N., Martin, R.V., Logan, J.A., Higurashi, A. and Nakajima, T., 2002: Tropospheric aerosol optical thickness from the GOCART Model and comparisons with satellite and sun photometer measurements, *Journal of Atmospheric Sciences*, 59(3), 461-483.
- Cosijn, C. and Tyson, P.D., 1996: Stable discontinuities in the atmosphere over South Africa, *South African Journal of Science*, 92, 381-386.
- de Villiers, M.G., Dutkiewicz, R.K. and Wicking-Baird, M.C., 1997: The Cape Town brown haze study, *Journal of Energy in Southern Africa*, 121-125.
- Draxler, R.R. and Hess, G.D., 1998: *Description of the HYSPLIT_4 modelling system*, NOAA Technical Memorandum ERL ARL-224, Silver Springs, Maryland.
- Dubovik, O., Holben, B., Eck, T.F., Smirnov, A., Kaufman, Y.J., King, M.D., Tanre, D. and Slutsker, I., 2002: Variability of absorption and optical properties of key aerosol types observed in worldwide locations, *Journal of Atmospheric Sciences*, 59(3), 590-619.

- Eck, T.F., Holben, B.N., Ward, D.E., Dubovik, O., Reid, J.S., Smirnov, A., Mukelabai, M.M., Hsu, N.C., O'Neill, N.T. and Slutsker, I., 2001: Characterization of the optical properties of biomass burning aerosols in Zambia during the 1997 ZIBBEE field campaign, *Journal of Geophysical Research*, 106, 3425-3448.
- Eck, T.F., Holben, B.N., Ward, D.E., Mukelabai, M.M., Dubovik, O., Smirnov, A., Schafer, J.S., Hsu, N.C., Piketh, S.J., Queface, A.J., le Roux, J., Swap, R.J. and Slutsker, I., 2003: Variability of biomass burning aerosol optical characteristics in southern Africa during the SAFARI 2000 dry season campaign and a comparison of single scattering albedo estimates from radiometric measurements, *Journal of Geophysical Research*, 108, 8477-8490.
- Facchini, M.C., Mircea, M., Fuzzi, S. and Charlson, R.J., 1999: Cloud albedo enhancement by surface-active organic solutes in growing droplets, *Nature*, 401(6750), 257-259.
- Formenti, P., Winkler, H., Fourie, P., Piketh, S.J., Makgopa, B., Helas, G. and Andreae, M.O., 2002: Aerosol optical depth over a remote semi-arid region of South Africa from spectral measurements of daytime solar extinction and the night time stellar extinction, *Atmospheric Research*, 62, 11-32.
- Freiman, M.T. and Piketh, S.J., 2003: Air transport in and out of the industrial Highveld region of South Africa, *Journal of Applied Meteorological Science*, 42, 994-1001.
- Freiman, M.T. and Tyson, P.D., 2000: The thermodynamic structure of the atmosphere over South Africa: implications for water vapour transport, *WaterSA*, 26(2), 153-158.
- Garstang, M., Tyson, P.D., Swap, R., Edwards, M., Kallberg, P. and Lindesay, J.A., 1996: Horizontal and vertical transport of air over Southern Africa, *Journal of Geophysical Research*, 101 (D19), 23721-23723 and 23736.

- GLOBE: Aerosol Protocol 2002: <<http://www.globe.gov>
 Website accessed: 02 June 2003.
- Hansen, J., Sato, M. and Ruedy, R., 1997: Radiative forcing and climate response, *Journal of Geophysical Research*, 102, 6831-6864.
- Harrison, M.S.J., 1984: The annual rainfall cycle over the central interior of South Africa, *South African Geographical Journal*, 66, 47-64.
- Held, G., Gore, B.J., Surridge, A.D., Tosen, G.R., Turner, C.R. and Walmsley, R.D. (Eds.) 1996: *Air pollution and its impact on the South African Highveld*, Environmental Scientific Association, Cleveland.
- Herring, P., 2002: *The biology of the deep ocean*. Oxford University Press, United Kingdom.
- Hinds, W.C., 1982: *Aerosol technology: Properties, behaviour and measurements of airborne particles*. John Wiley and Sons, Toronto.
- Holben, B.N., Eck, T.F., Slutsker, I., Tanré, D., Buis, J.P., Setzer, A., Vermote, E., Reagan, J.A., Kaufman, Y.J., Nakajima, T., Lavenue, F., Jankowiak, I. and Smirnov, A., 1998: AERONET- A federated instrument network and data archive for aerosol characterization, *Remote Sensing Environment*, 66, 1-16.
- Holben, B.N., Tanre, D., Smirnov, A., Eck, T.F., Slutsker, I., Abuhassan, N.W.W., Newcomb, N.N., Schafer, J.S., Chatenet, B., Lavenue F., Kaufman, Y.J., Van de Castle, J., Setzer, A., Markham, B., Clark, D., Frouin, R., Halthore, R., Karnieli, A., O'Neill, N.T., Pietras, C., Pinker, R.T., Voss, K. and Zibordi, G., 2001: An emerging ground based aerosol climatology: aerosol optical depth from AERONET, *Journal of Geophysical Research*, 106, 12067-12097.
- Houghton, J.T., Meira Filho, L.G., Bruce, J., Lee, H., Callander, B.A., Haites, E., Harris, N. and Maskell, K. (Eds.), 1995: *Climate change 1994: Radiative forcing of climate change and an evaluation of the IPCC IS92 emission scenarios*, Cambridge University Press, New York.

- Houghton, J.T., Ding, Y., Griggs, D.J., Noguer, M., Van der Linden, P.J., Dai, X., Maskell, K. and Johnson, C.A. (Eds.), 2001: *The climate system: An overview*, Cambridge University Press, New York.
- IPCC., 2001: "Climate change: The scientific basis". In: *The climate system: An overview*, Houghton, J.T., Ding, Y., Griggs, D.J., Noguer, M., Van der Linden, P.J., Dai, X., Maskell, K. and Johnson, C.A. (Eds.), Cambridge University Press, New York.
- Iqbal, M., 1983: *An introduction to solar radiation*, Academic Press, Toronto.
- Levine J.S. (Ed.), 1996: *Biomass Burning and Global Change*, MIT Press, Cambridge, Massachusetts.
- Levine, J.S. (Ed.), 1996: *Global Biomass Burning: Atmospheric, Climate and Biospheric Implications*, MIT Press, Cambridge, Massachusetts.
- Maenhaut, W., Salma, I., Cafmeyer, J., Annegarn, H.J. and Andreae, M.O., 1996: Regional atmospheric aerosol composition and sources in the Eastern Transvaal, South Africa and impacts of biomass burning, *Journal of Geophysical Research*, 101, 23631-23650.
- NASA (National Aeronautical Space Administration), 2002: *Terra - Detection of global change and its causes*,
http://terra.nasa.gov/Brochure/sect_3-2.html
 Website accessed: 12 November 2003.
- Newcomb, W., 2003: Personal communication via Dr Tal Freiman. NASA Goddard Flight Space Centre, Maryland.
- O'Neill, N.T., Eck, T.F., Holben, B.N., Smirnov, A. and Dubovik, O., 2001: Bimodal size distribution influences on the variation of Ångström derivatives in spectral and optical depth space, *Journal of Geophysical Research*, 106, 9787-9806.
- OECD (Organisation for Economic Co-operation and Development), 1999: *Energy, the next fifty years*, OECD Publications Service, Paris, France.

- Ogren, J.A., 1995: “A systematic approach to *in situ* observations of aerosol properties”. In: *Aerosol Forcing of Climate*, R.J. Charlson and J. Heintzenberg (Eds.), John Wiley and Sons, New York, 230-250.
- Piketh, S.J., 1995: *Generation and transportation characteristics of suspended particles in the Eastern Transvaal*, Unpublished MSc dissertation, University of the Witwatersrand, Johannesburg.
- Piketh, S.J., Annegarn, H.J. and Kneen, M.A., 1996: “Regional scale impacts of biomass burning emissions over southern Africa”. In: *Biomass Burning and Global Change*, Levine J.S. (Ed.), MIT Press, Cambridge, Massachusetts. 320-326.
- Piketh, S.J., Swap, R.J., Anderson, C.A., Freiman, M.T., Zunckel, M. and Held, G., 1999: The Ben Macdhuigh high altitude trace gas and aerosol transport experiment, *South African Journal of Science*, 95, 35-43.
- Queface, A.J., Piketh, S.J., Annegarn, H.J., Holben, B.N. and Uthui, R.J., 2003: Retrieval of aerosol optical thickness and size distribution from the Cimel sun photometer over Inhaca Island, Mozambique, *Journal of Geophysical Research*, 108, 8509-8519.
- Raes, F., Wilson, J. and Vandingenen, R., 1995: “Aerosols dynamics and its implications for the global aerosol”. In: *Aerosol Forcing of Climate*, R.J. Charlson and J. Heintzenberg (Eds.), John Wiley and Sons, New York, 120-131.
- Rorich, R.P. and Galpin, J.S., 1998: Air quality in the Mpumalanga Highveld region, South Africa, *South African Journal of Science* 94, 109-114.
- Salma, I., Maenhaut, W., Cafmeyer, J., Annegarn, H.J. and Andreae, M.O., 1992: PIXE analysis of cascade impactor samples collected at the Kruger National Park, South Africa, *Nuclear Instruments and Methods in Physics Research*, B 85, 845-855.

- Schafer, J.S., Holben, B.N., Eck, T.F., Yamasoe, M.A. and Artaxo, P., 2002: Atmospheric effects on insolation in the Brazilian Amazon: observed modification of solar radiation by clouds and smoke and derived single scattering albedo of fire aerosols, *Journal of Geophysical Research*, 107, 8074.
- Schulze, B.R., 1965: *Climate of South Africa: General Survey*. WB28. South African Weather Bureau, Pretoria, pg 330.
- Sokolik, I.N. and Toon, O.B., 1996: Direct radiative forcing by anthropogenic airborne mineral aerosol, *Nature*, 381, 681-683.
- Sokolik, I.N., Andronove, A. and Johnson, T.C., 1993: Complex refractive index of atmospheric dust aerosols, *Atmospheric Environment*, 27A, 2495-2502.
- Spalding-Fecher, R., Afrane-Okese, Y., Davis, M. and Matibe, K., 2000: *Electricity and the environment: World Wildlife Fund macroeconomic reforms and sustainable development in Southern Africa*, Energy and Development Research Centre, No. 5, University of Cape Town, Cape Town, 34-40.
- Swap, R.J., and Tyson, P.D., 1999: Stable discontinuities as determinants of the vertical distribution of aerosols and trace gases in the atmosphere, *South African Journal of Science*, 95, 63-71.
- Terblanche, D.E., Mittermaier, M.P., Burger, R.P., Piketh, S.J. and Bruintjes, R.T., 2000: The Aerosol Recirculation and Rainfall Experiment (ARREX): an initial study on aerosol-cloud interactions over South Africa, *South African Journal of Science*, 96, 15-22.
- Turner, C.R., 1990: *A five year study of air quality in the Highveld region*, Eskom Report no. TRR/S90/002, Eskom TRI, Johannesburg.
- Tyson, P.D. and Preston-Whyte, R.A., 2000: *The weather and climate of Southern Africa*. Oxford University Press, Cape Town.

- Tyson, P.D., 1999: Atmospheric transport of aerosols and trace gases over Southern Africa, *Progress in Physical Geography*, 21, 79-101.
- Tyson, P.D., Garstang, M., Swap, R., Kallberg, P. and Edwards, M., 1996: An air transport climatology for subtropical Southern Africa, *International Journal of Climatology*, 16, 265-291.
- Tyson, P.D., Landman, A., Mason, S.J. and Tennant, W.J., 2000: Retro-active skill of multi-tiered forecasts of summer rainfall over southern Africa, *International Journal of Climatology*, 21, 1-19.
- Väkeva, M., Hämer, K., Kulmala, M., Lahdes, R., Ruuskanen, J. and Laitinen, T., 1999: Street level versus rooftop concentrations of sub-micron aerosol particles and gaseous pollutants in an urban street canyon, *Atmospheric Environment*, 33, 1385-1397.
- Visser, M., Spalding-Fecher, R., and Leiman, A., 1999: *Manufacturing and economic growth*. Energy and Development Research Centre, University of Cape Town, Cape Town, pg 23-40.
- Wentzel, M., Annegarn, H.J., Helas, G., Weinbruch, S., Balogh, A.G. and Sithole, J.S., 1999: Giant dendritic carbonaceous particles in Soweto aerosols, *South African Journal of Science*, 95, 141-146.